BIOCHEMISTRY
including biophysical chemistry & molecular biology

Current Topic

pubs.acs.org/biochemistry

Membrane Protein Structure Determination Using Crystallography and Lipidic Mesophases: Recent Advances and Successes

Martin Caffrey,* Dianfan Li, and Abhiram Dukkipati

Membrane Structural and Functional Biology Group, School of Medicine and School of Biochemistry and Immunology, Trinity College Dublin, Dublin, Ireland

ABSTRACT: The crystal structure of the β_2-adrenergic receptor in complex with an agonist and its cognate G protein has just recently been determined. It is now possible to explore in molecular detail the means by which this paradigmatic transmembrane receptor binds agonist, communicates the impulse or signaling event across the membrane, and sets in motion a series of G protein-directed intracellular responses. The structure was determined using crystals of the ternary complex grown in a rationally designed lipidic mesophase by the so-called *in meso* method. The method is proving to be particularly useful in the G protein-coupled receptor field where the structures of 13 distinct receptor types have been determined in the past 5 years. In addition to receptors, the method has proven to be useful with a wide variety of integral membrane protein classes that include bacterial and eukaryotic rhodopsins, light-harvesting complex II (LHII), photosynthetic reaction centers, cytochrome oxidases, β-barrels, an exchanger, and an integral membrane peptide. This attests to the versatility and range of the method and supports the view that the *in meso* method should be included in the arsenal of the serious membrane structural biologist. For this to happen, however, the reluctance to adopt it attributable, in part, to the anticipated difficulties associated with handling the sticky, viscous cubic mesophase in which crystals grow must be overcome. Harvesting and collecting diffraction data with the mesophase-grown crystals are also viewed with some trepidation. It is acknowledged that there are challenges associated with the method. Over the years, we have endeavored to establish how the method works at a molecular level and to make it user-friendly. To these ends, tools for handling the mesophase in the pico- to nanoliter volume range have been developed for highly efficient crystallization screening in manual and robotic modes. Methods have been implemented for evaluating the functional activity of membrane proteins reconstituted into the bilayer of the cubic phase as a prelude to crystallogenesis. Glass crystallization plates that provide unparalleled optical quality and sensitivity to nascent crystals have been built. Lipid and precipitant screens have been designed for a more rational approach to crystallogenesis such that the method can now be applied to an even wider variety of membrane protein types. In this work, these assorted advances are outlined along with a summary of the membrane proteins that have yielded to the method. The prospects for and the challenges that must be overcome to further develop the method are described.

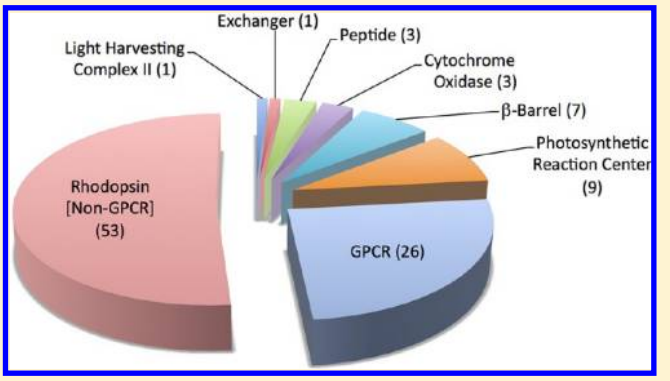

Whenever M. Caffrey teaches a course on introductory biochemistry, he suggests that the students come up with their own definition of biochemistry and encourages them to reflect on that definition at the end of term in light of the material covered. At the same time, he offers his own somewhat contrived definition, an abbreviated version of which is that biochemistry is the scientific endeavor that seeks to establish how an organism produces the right chemicals in the right place at the right time and in the right amounts. It is contrived in the sense that it is used to alert the students to the range of topics that will be covered. The definition includes the word "how", which is there to introduce the concepts of mechanism and function. By relating these to structure, he is able to engage the students in a discussion of how structure relates to function or activity and to describe the myriad ways in which biomolecular structure is revealed.

In that discussion of structure and function, the treatment is usually broadened to include the work of L. Sullivan who, in reference to buildings and architecture, introduced the dictum "form ever follows function". The concept is nicely illustrated by considering the amphitheaters and odeons of old, designed for effective communication of one or a few with many. In the biological world, the form, or structure, and function relationship can be viewed in a similar light. However, the directionality is a little different in that usually what we seek, as biochemists and structural biologists, is insight into function as revealed by knowing the structure of the corresponding biomolecule, usually a protein. By structure is meant the arrangement in three-dimensional space and the connectivity of all (usually non-hydrogen) atoms in the protein. Insight has two primary uses. One is to establish the chemical, physical, and structural or spatial bases of a particular function or activity. An

Received: January 4, 2012
Revised: July 11, 2012
Published: July 11, 2012

dx.doi.org/10.1021/bi300010w | *Biochemistry* 2012, 51, 6266−6288

activity could be a reaction catalyzed by an enzyme, the creation of an ion gradient, or the binding of a ligand leading to signal transduction by a receptor. The other is the exploitation of such understanding, for the purpose of rational drug design, for example.

For the level of detail required, the structure revealing method most relevant to integral membrane proteins, the focus of this work, is macromolecular X-ray crystallography (MX). To perform a successful MX study, however, diffraction-quality three-dimensional crystals of the target protein are needed. There are several methods by which to crystallize membrane proteins, and these are divided here into two major categories. The first and most successful, hereafter termed the *in surfo* method,[1] was introduced some three decades ago.[2] It uses surfactants to produce mixed micelles that incorporate the pure target protein, residual lipid if present, and detergent. These soluble protein−detergent complexes, with or without added small amphiphiles, are treated in essentially the same way as water-soluble proteins for the production of crystals by vapor diffusion, counter diffusion, microdialysis, or batch methods. The target protein can originate from native membranes, from the membranes or inclusion bodies of recombinant organisms, from cell-free expression,[3,4] or from chemical synthesis.[5]

Difficulties in crystallizing membrane proteins by the *in surfo* approach have been attributed to inherent protein flexibility and to conformational inhomogeneity. At fault too can be the relatively diminutive polar surface that is simply too small to extend beyond the surfactant swath and to make lasting molecular contacts with neighboring proteins in the crystal. Shorter chain detergents and amphiphile additives have been used to advantage here.[2,6] Protein fusions,[7−23] antibodies,[12,24−27] and designed ankyrin repeat protein binders[28] have been introduced, which also make good these deficits. They can be tailored, to a degree, to create stable protein−protein polar contacts within the crystal. Furthermore, by using high-affinity recombinant antibodies raised against a discontinuous epitope on the native protein surface, flexibility in the protein−antibody complex cocrystal is minimized and conformational homogeneity is favored. All contribute to producing a well-diffracting crystal. These technically challenging approaches have been used successfully in structure studies of cytochrome *c* oxidase,[29] the cytochrome bc_1 complex (with and without cytochrome *c*),[24] ion channels,[30−35] transporters,[36] G protein-coupled receptors (GPCRs),[25,26,37] and a receptor−Gs protein complex.[12]

The second category of membrane protein crystallization methods includes those that make use of a lipidic bicontinuous mesophase,[38−40]a discoidal lipid/detergent bicelle,[41] or vesicle fusion.[42] In all three cases, an extended bilayer composed of lipid, detergent, and target protein is presumed to form. For this reason, these are here collectively termed the bilayer methods of membrane protein crystallization. Unfortunately, we know little of the molecular mechanism whereby crystals form by the assorted *in surfo* protocols. Accordingly, the possibility that a bilayered structure also forms as an intermediate in the crystallization pathway that begins with a solution of mixed micelles in the *in surfo* method cannot be excluded. The focus of the rest of this work is on the method that employs a lipidic mesophase, the cubic phase in particular. This is hereafter termed the *in meso* method. It is proving to be a useful approach for crystallizing a broad range of membrane protein types (Table 1), having been used with extraordinary success recently for GPCRs (Table 2). The cubic phase is a lyotropic liquid crystal.[43,44] It consists of a highly curved lipid bilayer, the midplane of which is draped over a periodic minimal surface with cubic symmetry. The bilayer separates two interpenetrating but noncontacting aqueous channels. Both the aqueous and bilayer compartments are continuous in three dimensions. As a result, the mesophase is described as being bicontinuous (Figure 1).

The *in meso* method is particularly appealing because it offers the prospect that crystallization takes place from within a lipid bilayer, akin to the native environment encountered in a biomembrane. This is in contrast to the more traditional *in surfo* crystallogenesis methods that involve using potentially destabilizing surfactant micelles. Our research team, in the Membrane Structural and Functional Biology (MS&FB) Group, has been working on the *in meso* method since its introduction in the late 1990s.[43] The thrust of our work in this area has three major themes: (1) to decipher the molecular basis of *in meso* crystallogenesis, (2) to automate and miniaturize the method and to make it more user-friendly and generally accessible, and (3) to use the method to determine the structures of membrane proteins that are critical to human health. In what follows, the origins of the *in meso* method, its development as a high-throughput technique, the membrane proteins that have yielded to it, and the prospects and the challenges ahead are described. Practical and strategic issues that the membrane protein crystallographer might consider ahead of launching into and during the course of *in meso* crystallization trials are summarized in Chart 1.

EXPERIMENTAL ASPECTS

Performing an *in meso* crystallization trial is simple and straightforward. Typically, it involves combining two parts protein solution with three parts lipid at 20 °C.[45,46a] The lipid most commonly used is the monoacylglycerol (MAG), monoolein (9.9 MAG).[a] According to the monoolein/water phase diagram (Figure 2B),[48] and assuming there is no major influence on the phase behavior of the protein solution components, this mixing process should generate, by spontaneous self-assembly, the cubic mesophase (Figure 2) at or close to full hydration. The pure cubic phase is colorless, optically isotropic (nonbirefringent), transparent, and viscous. The last three characteristics can be used conveniently to indicate that the proper phase has been accessed.[b]

The cubic phase is sticky and viscous akin to thick toothpaste. Without the proper tools, it is not particularly easy to handle. In the course of earlier lipid phase science work in the MS&FB Group, we had developed tools (Figure 3) and procedures for preparing and manipulating such rheologically refractory materials. One of these, the coupled syringe mixing device,[49] was ideally suited to the task of combining microliter volumes of lipid with a membrane protein solution in a way that produces protein-laden mesophase for direct use in crystallization trials with minimal waste and change in composition. The mixer consists of two Hamilton microsyringes connected by a narrow bore coupler. Lipid is placed in one syringe and protein solution in the other. Mixing is achieved by repeatedly moving the contents of the two syringes back and forth through the coupler.[46a] The coupler is replaced with a needle for convenient dispensing of the homogeneous mesophase into wells of custom-designed glass sandwich crystallization plates.[50,51] Precipitant solutions of varying compositions are placed over the mesophase, and the wells are sealed with a cover glass. The plates are incubated at 20 °C

Table 1. *In Meso* Structures of Non-GPCR Membrane Proteins and Peptides

protein (organism) (PDB record count)[a]	protein size (no. of amino acids)[b]	detergent[c,d]	[protein] (mg/mL)[e]	hosting lipids[c,f]	PDB entry[g] (resolution (Å)) (solvent content (%))
β-helix					
gramicidin D (*Brevibacillus brevis*) (3)	15	not applicable	130	7.7 MAG, 8.8 MAG, 9.9 MAG	2Y5M (1.08) (52.3), 2Y6N (1.26) (52.0), 2XDC (1.70) (51.0)
β-barrel					
ButB (*Escherichia coli*) (1)	594	LDAO	15	9.9 MAG	2GUF (1.95) (53.1)
OpcA (*Neisseria meningitidis*) (1)	253	DDM	12	9.9 MAG	2VDF (1.95) (43.0)
OmpF (*E. coli*) (3)	340	DDM	10−55	9.9 MAG	3POQ (1.90) (52.0), 3POX (2.00) (64.7), 3POU (2.80) (61.2)
intimin (*E. coli*) (1)	242	LDAO	20	9.9 MAG	4E1S (1.86) (50.1)
invasin (*Yersinia pseudotuberculosis*) (1)	245	LDAO	20	9.9 MAG	4E1T (2.26) (57.6)
α-helical					
bacterorhodopsin (*Halobacterium salinarum*) (38)	248	OG	10−30	9.9 MAG, β-XylOC$_{16+4}^{h}$	1M0K (1.43) (42.1), 1M0M (1.43) (41.3), 1M0L (1.47) (41.3), 1P8H (1.52) (30.8), 2NTU (1.53) (44.1), 2NTW (1.53) (44.1), 1C3W (1.55) (53.2), 1O0A (1.62) (42.4), 1P8U (1.62) (30.9), 1KGB (1.65) (46.9), 1F50 (1.70) (46.7), 3NS0 (1.78) (36.6), 3NSB (1.78) (43.9), 1C8R (1.80) (42.3), 1F4Z (1.80) (46.7), 1KG9 (1.81) (46.9), 2I21 (1.84) (44.0), 1P8I (1.86) (32.3), 1QHJ (1.90) (48.0), 1C8S (2.00) (54.2), 1KG8 (2.00) (46.0), 2I1X (2.00) (47.9), 1JV6 (2.00) (43.7), 1MGY (2.00) (43.7), 3MBV (2.00) (44.7), 2I20 (2.08) (44.1), 1E0P (2.10) (51.0), 1QKO (2.10) (48.0), 1QKP (2.10) (48.0), 2WJL (2.15) (33.1), 1CWQ (2.25) (null[i]), 1JV7 (2.25) (52.1), 1BRX (2.30) (43.1), 2WJK (2.30) (35.5), 1S8J (2.30) (48.7), 1S8L (2.30) (47.2), 1VJM (2.30) (46.7), 1AP9 (2.35) (48.0)
halorhodopsin (*H. salinarum*) (3)	274	OG	8−10	9.9 MAG	2JAF (1.70) (47.4), 1E12 (1.80) (41.5), 2JAG (1.93) (48.2)
sensory rhodopsin II (*Natronomonas pharaonis*) (6)	217	DDM	11.2	9.9 MAG	3QAP (1.90) (55.8), 1H68 (2.10) (null[i]), 1GU8 (2.27) (53.0), 1GUE (2.27) (53.0), 1JGJ (2.40) (60.8), 3QDC (2.50) (57.0)
sensory rhodopsin II−transducer complex (*N. pharaonis*) (3)	225 + 82, 248 + 122, 248 + 163	OG	not available	11.7 MAG	1H2S (1.93) (null[i]), 2F93 (2.00) (38.9), 2F95 (2.20) (31.6)
sensory rhodopsin (*Nostoc* sp. PCC 7120) (1)	261	DDM	9	9.9 MAG	1XIO (2.00) (55.9)
channelrhodopsin (*Chlamydomonas reinhardtii*) (1)	333	DDM	10	9.9 MAG	3UG9 (2.30) (50.6)
Acetabularia rhodopsin II (*Acetabularia acetabulum*) (1)	229	DDM	45.4	9.9 MAG with 10% (w/w) cholesterol	3AM6 (3.20) (58.1)
light-harvesting complex II (*Rhodoblastus acidophilus*) (1)	(53 + 41) × 9	LDAO	10	9.9 MAG	2FKW (2.45) (66.0)
photosynthetic reaction center (*Blastochloris viridis*) (5)	336 + 258 + 274 + 324	LDAO	20−25	9.9 MAG	2WJN (1.86) (54.0), 2WJM (1.95) (54.0), 2X5U (3.00) (54.0), 2X5V (3.00) (68.7), 4AC5 (8.20) (64.0)
photosynthetic reaction center (*Rhodobacter sphaeroides*) (4)	235 + 281 + 300, 250 + 281 + 307, 281 + 307 + 260, 281 + 307 + 260	LDAO	20−25	9.9 MAG	2GNU (2.20) (51.6), 1OGV (2.35) (55.6), 2BNS (2.50) (59.1), 2BNP (2.70) (55.6)

dx.doi.org/10.1021/bi300010w | *Biochemistry* 2012, 51, 6266−6288

Table 1. continued

protein (organism) (PDB record count)[a]	protein size (no. of amino acids)[b]	detergent[c,d]	[protein] (mg/mL)[e]	hosting lipids[c,f]	PDB entry[g] (resolution (Å)) (solvent content (%))
ba_3 cytochrome *c* oxidase (*Thermus thermophilus*) (2)	569 + 168 + 34	DDM	15	9.9 MAG	3S8F (1.80) (60.8), 3S8G (1.80) (61.7)
caa_3 cytochrome *c* oxidase (*T. thermophilus*) (1)	791 + 337 + 66	DM	10	7.7 MAG	2YEV (2.36)
Na^+-Ca^{2+} exchanger (*Methanocaldococcus jannaschii*) (1)	320	DM	10	9.9 MAG	3V5U (1.90) (51.5)

[a]As of July 2012, the total count of non-GPCR structure records in the PDB attributable to the *in meso* method was 77. For GPCRs, the total count is 26. [b]Protein size refers to the number of amino acid residues in the protein. Where the protein consists of multiple subunits or protomers, the number of residues in each is provided. Protein size information is listed in the same order as the corresponding PDB entry. [c]Abbreviations used for detergents and lipids: LDAO, lauryldimethylamine *N*-oxide; DDM, *n*-dodecyl β-D-maltopyranoside; DM, *n*-decyl β-D-maltopyranoside; OG, *n*-octyl β-D-glucopyranoside; b-XylOC$_{16+4}$, 1-O-(3,7,11,15-tetramethylhexadecyl)-β-D-xyloside. [d]This refers to the detergent in which the protein was solubilized prior to its use in creating the protein-laden mesophase for *in meso* crystallogenesis. [e]Refers to the protein concentration of the solution used to prepare the hosting mesophase with one exception. In the case of gramicidin, the concentration refers to the peptide concentration in the mesophase after reconstitution. [f]Refers to the composition of the lipid used to prepare the hosting mesophase. Where different hosting lipids are used with a single protein, their identities are given in the same order as the corresponding PDB entries. [g]PDB records are linked to the corresponding record in the Membrane Protein Data Bank (http://www.mpdb.tcd.ie), which links to the PDB and to other useful sites. [h]This lipid was used in the work associated with PDB entry 3MBV. [i]Null is used in the PDB to indicate that the relevant information is not available.

and monitored for crystal growth. Optical quality is the best it can be, given that the mesophase is sandwiched between two glass plates and the mesophase itself, ideally, is transparent. This means that crystals, just a few micrometers in size, can be seen readily with a high-quality microscope, whether or not the protein is colored. The use of cross-polarizers can help with visualizing small crystals that usually appear birefringent on a dark background; as noted, the cubic phase itself is optically isotropic and nonbirefringent. If the target protein is naturally colored or has been labeled with a colored or fluorescent tag,[52,53] visibility will be enhanced. However, it is important to stress that crystals of colorless protein are readily seen in sandwich plates (Figure 4).[45,46a] An added feature of the glass sandwich plate is that the double-sided tape used to create the wells provides almost hermetic sealing ensuring minimal change in well contents during the course of trials that can last for months. Step-by-step instructions, complete with an online video demonstration of the entire *in meso* crystallization process just described, have been published.[45,46a] Additional video articles illustrating harvesting[46b] and use of a robot are available.[46c]

PROPOSED MOLECULAR MECHANISM

Model. A proposal has been advanced for how *in meso* crystallogenesis takes place at the molecular level (Figure 5).[1,43,44,54] It begins typically with an isolated biological membrane that is treated with detergent to solubilize the target protein. The protein−detergent complex is purified by standard wet-lab biochemical methods. Homogenizing with a MAG effects a uniform reconstitution of the purified protein into the bilayer of the cubic phase. As noted, the latter is bicontinuous in the sense that both the aqueous and bilayer compartments are continuous in three-dimensional space (Figure 1). Upon reconstitution, the protein ideally retains its native conformation and activity and has partial or complete mobility within the plane of the cubic phase bilayer. A precipitant is added to the mesophase, which triggers a local alteration in mesophase properties that include phase identity, microstructure, long-range order, and phase separation. Under conditions leading to crystallization, one of the separated phases is enriched in protein, which nucleates and develops into a bulk crystal. The hypothesis envisions a local lamellar phase that acts as a medium in which nucleation and three-dimensional crystal growth occur. Molecular dynamics simulations highlight the hydrophobic−hydrophilic mismatch between the protein and the surrounding bilayer in the lamellar phase as a driving force for oligomerization in the membrane plane.[55] The local lamellar phase also serves as a conduit or portal for proteins on their way from the cubic phase reservoir to the growing face of the crystal. Initially at least, the proteins leave the lamellar conduit and ratchet into the developing crystal to generate a layered-type (type I)[2] packing of protein molecules (Figures 5 and 6). Given that proteins reconstitute across the bilayer of the cubic phase with no preferred orientation and the three-dimensional continuity of the mesophase, it is possible for the resulting crystals to be polar or nonpolar.[44] These correspond to situations in which adjacent proteins in a layer have their long-axis director oriented in the same direction or in opposite directions.

The proposal for how nucleation and crystal growth occur *in meso* relies absolutely on the three-dimensional continuity of the mesophase. Under the assumption that the sample exists as a single liquid crystallite or monodomain, continuity ensures

Table 2. *In Meso* Structures of G Protein-Coupled Receptors and Receptor Complexes

receptor (pharmacological state)	ligand[a]	covalent/noncovalent partner	detergent/lipid[b]	[protein][c] (mg/mL)	hosting lipid[d]	PDB entry[e] (resolution (Å)) (solvent content (%))
μ-opioid (inactive)	β-FNA	T4 lysozyme	MNG-DDM/CHS	30	9.9 MAG with 10% (w/w) cholesterol	4DKL (2.80) (67.8)
κ-opioid (inactive)	JDTic	T4 lysozyme	DDM/CHS	40	9.9 MAG with 10% (w/w) cholesterol	4DJH (2.90) (67.8)
nociceptin (inactive)	Compound-24	apo-cytochrome b_{562}RIL	DDM/CHS	40	9.9 MAG with 10% (w/w) cholesterol	4EA3 (3.01) (48.4)
δ-opioid (inactive)	Naltrindole	T4 lysozyme	MNG/CHS	50	9.9 MAG with 10% (w/w) cholesterol	4EJ4 (3.40) (69.3)
sphingosine 1-phosphate subtype 1 (inactive)	ML056	T4 lysozyme	DDM/CHS	100	9.9 MAG with 10% (w/w) cholesterol	3V2Y (2.80) (52.9)
	ML056	T4 lysozyme	DDM/CHS	100	9.9 MAG with 10% (w/w) cholesterol	3V2W (3.35) (52.9)
muscarinic acetylcholine M2 (inactive)	QNB	T4 lysozyme	MNG	50	9.9 MAG with 10% (w/w) cholesterol	3UON (3.00) (57.7)
muscarinic acetylcholine M3 (inactive)	Tiotropium	T4 lysozyme	MNG/CHS	60	9.9 MAG with 10% (w/w) cholesterol	4DAJ (3.40) (54.2)
histamine H1 (inactive)	Doxepin	T4 lysozyme	DDM/CHS	40	9.9 MAG with 10% (w/w) cholesterol	3RZE (3.10) (60.0)
dopamine D3 (inactive)	Eticlopride	T4 lysozyme	DDM/CHS	30	9.9 MAG with 10% (w/w) cholesterol	3PBL (3.15) (63.5)
CXCR4 chemokine (inactive)	IT1t	T4 lysozyme	DDM/CHS	60−70	9.9 MAG with 10% (w/w) cholesterol	3ODU (2.50) (55.8)
	CVX15	T4 lysozyme	DDM/CHS	60−70	9.9 MAG with 10% (w/w) cholesterol	3OE0 (2.90) (66.0)
	IT1t	T4 lysozyme	DDM/CHS	60−70	9.9 MAG with 10% (w/w) cholesterol	3OE8 (3.10) (55.8)
	IT1t	T4 lysozyme	DDM/CHS	60−70	9.9 MAG with 10% (w/w) cholesterol	3OE9 (3.10) (60.3)
	IT1t	T4 lysozyme	DDM/CHS	60−70	9.9 MAG with 10% (w/w) cholesterol	3OE6 (3.20) (58.0)
A_{2A} adenosine (inactive)	ZM241385	apo-cytochrome b_{562}RIL	DDM/CHS	60	9.9 MAG with 10% (w/w) cholesterol	4EIY (1.80) (50.50)
	ZM241385	T4 lysozyme	DDM/CHS	70	9.9 MAG with 10% (w/w) cholesterol	3EML (2.60) (56.79)
A_{2A} adenosine (active)	UK-432097	T4 lysozyme	DDM/CHS	60	9.9 MAG with 10% (w/w) cholesterol	3QAK (2.70) (58.11)
β_2-adrenergic (inactive)	Carazolol	T4 lysozyme	DDM/CHS	50	9.9 MAG with 10% (w/w) cholesterol	2RH1 (2.40) (59.98)
	Timolol	T4 lysozyme	DDM/CHS	30	9.9 MAG with 10% (w/w) cholesterol	3D4S (2.80) (47.36)
	not available	T4 lysozyme	DDM/CHS	>60	9.9 MAG with 10% (w/w) cholesterol	3NY9 (2.80) (48.68)
	ICI 118,551	T4 lysozyme	DDM/CHS	>60	9.9 MAG with 10% (w/w) cholesterol	3NY8 (2.84) (49.02)
	Alprenolol	T4 lysozyme	DDM/CHS	>60	9.9 MAG with 10% (w/w) cholesterol	3NYA (3.10) (48.33)
	FAUC50[f]	T4 lysozyme	MNG-3	50	9.9 MAG with 10% (w/w) cholesterol	3PDS (3.50) (65.00)
β_2-adrenergic Gs protein complex (active)	BI-167107	T4 lysozyme/Nanobody 35	MNG-3	not available	7.7 MAG with 10% (w/w) cholesterol	3SN6 (3.20) (60.05)
β_2-adrenergic (active)	BI-167107	T4 lysozyme/Nanobody 80	MNG-3	not available	9.9 MAG with 10% (w/w) cholesterol	3P0G (3.50) (53.97)

[a]Ligands are reported as in the source article. [b]Abbreviations for detergents and lipids: DDM, *n*-dodecyl β-D-maltopyranoside; CHS, cholesteryl hemisuccinate; MNG, maltose-neopentyl glycol. [c]Refers to the protein concentration in the solution used to prepare the hosting mesophase. [d]Refers to the composition of the lipid used to prepare the hosting mesophase. [e]PDB records are linked to the corresponding record in the Membrane Protein Data Bank (http://www.mpdb.tcd.ie), which links to the PDB and to other useful sites. [f]FAUC50 is a covalently bound agonist.

that the mesophase acts essentially as an infinite reservoir from which all protein molecules in the sample can end up in a bulk crystal. Neither the lamellar liquid crystal (L_α) nor the inverted hexagonal (H_{II}) phase, each of which is an accessible mesophase in lipidic systems (Figure 2), has three-dimensional continuity and alone is unlikely to support membrane protein crystallogenesis by the *in meso* method.[44]

Because of the proposed need for the diffusion of proteins in the bilayer and of precipitant components in the aqueous channels of the mesophase, the expectation is that crystal growth rates might be tardy *in meso*. However, crystals have been seen to form within 1 h,[c] which suggests that the slowness associated with restricted diffusion can be offset by a reduction in dimensionality. The latter is a result of the protein being confined to a lipid bilayer with its long axis oriented perpendicular to the membrane plane. Thus, the number of orientations that must be sampled to effect nucleation and crystal growth is small *in meso* compared with the number in its

dx.doi.org/10.1021/bi300010w | *Biochemistry* 2012, 51, 6266−6288

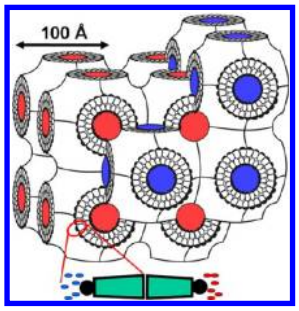

Figure 1. Cartoon representation of a bicontinuous lipidic cubic mesophase. At its simplest, the cubic phase is formed by homogenizing lipid, typically monoolein (9.9 MAG), and water in approximately equal parts at 20 °C. An expanded view of the lipid component that forms the continuous curved bilayer is shown at the bottom. Water channels, on either side of the bilayer, that interpenetrate but never contact one another as they permeate the mesophase are colored blue and red for the sake of clarity. The lattice parameter of the cubic phase, in this case in space group *Im3m*, obtained using small-angle X-ray scattering, is indicated.[48,131]

in surfo counterpart, in which all of the three-dimensional space is accessible.[2]

That crystal growth takes place in a mesophase implies it is happening in a convection-free environment. This is analogous to growth under conditions of microgravity or in a gel, which offers the advantage of a stable zone of depletion around the growing crystal and thus a slower and more orderly growth.[56] Settling of crystals and subsequent growth into one another are also avoided under these conditions, as is the likelihood that impurities are wafted in from the surrounding solution to poison the face of the crystal and limit growth. For all these reasons, *in meso* crystallogenesis is similar to crystallization in space with the prospect of producing high-quality, structure-grade crystals.

Evidence for the Model. Experimental evidence in support of aspects of the hypothesis outlined above follows.

Reconstitution. The *in meso* method begins with what is assumed to be a uniform reconstitution of the protein into the lipid bilayer of the cubic phase (Figure 5). The protein is combined with MAG, typically in a ratio that should produce the cubic phase provided the detergent concentration of the protein solution is not too high. When this was done with the vitamin B_{12} transporter BtuB,[57] the invasin/adhesin OpcA,[58] and gramicidin D,[59] for example, the expected cubic-Pn3m phase was produced as evidenced by small-angle X-ray scattering (SAXS). The lattice parameter of the cubic phase was similar to the value observed with control, protein-free samples. Upon addition of a precipitant solution to trigger nucleation and crystal growth in the case of BtuB, the cubic phase swelled and formed the sponge phase.[60] It is from this swollen, bicontinuous mesophase that the crystals of BtuB were harvested. These data are consistent with the view that the protein is reconstituted into the cubic phase in a way that is homogeneous and that does not perturb the original mesophase.

That reconstitution is uniform throughout the cubic mesophase is obvious when working with highly colored proteins such as bacteriorhodopsin,[38] the photosynthetic reaction center,[61] and light-harvesting complex II (LHII).[60] After the lipid and protein solution is homogenized, an optically clear mesophase is produced that, to the naked eye, is uniformly colored.

The electronic fluorescence properties of the gramicidin molecule directly reconstituted into the lipid bilayer of the cubic phase suggest that it resides in an apolar environment.[33] Thus, the yield and wavelength of maximal intensity of the fluorescence from the tryptophans in gramicidin were increased and blue-shifted, respectively, compared with those of tryptophan in an aqueous solution.

Quenching of intrinsic tryptophan fluorescence by a lipid with a dibrominated acyl chain (bromo-MAG) has been used to demonstrate reconstitution of BtuB,[57] OpcA,[58] diacylglycerol kinase (DgkA),[62] and gramicidin[59] in the lipidic mesophase. These have 13, 4, 5, and 4 tryptophans, respectively, of which

Chart 1. Issues To Consider When Undertaking an *in Meso* Crystallogenesis Study Assuming Little Prior Knowledge about the Crystallization Potential of the Membrane Protein Target[a]

Host Lipid: 9.9 MAG*, 7.7 MAG, 7.8 MAG, 7.9 MAG, 8.8 MAG, 9.7 MAG, others

Additive Lipid: none*, glycerophospholipid, neutral lipids, sphingolipids, sterols, lipid extracts/mixes

Protein Considerations:

immediate

- Concentration: highest possible* then reduce as needed. Be mindful of excess detergent
- Buffer: type and pH. Use values where protein is most stable
- Salt: type, concentration. Use values where protein is most stable

longer-term

- Engineering: truncation, insertion, fusion, stabilizing mutations
- Complexes: nanobody, antibody, designed ankyrin repeat, native partner
- Post-translational modification sites: glycosylation, phosphorylation, etc. Render uniform or mutate
- Block or mutate surface exposed free-cysteines
- Limited proteolysis
- Homologs

Ligands: Include known stabilizing ligands (substrates, products, analogs, inhibitors, activators, cofactors, prosthetic groups, ions) if available

Initial Screens: 10 commercial kits*, customized screens (GPCRs, β-barrels for example)

Optimization Screens: Focus grid screens around initial hit conditions. Follow up with additive screens (salts, sugars, amino acids, detergents, small molecules, acids/bases, polymers, etc.)

Temperature (°C): 20*, 4, 12

Screening Schedule: 0, 1, 2, 3, 5, 7 days, 2, 3, 4, 8, 12 weeks, 6 months, 1 year

[a]Items with an asterisk should be given priority.

dx.doi.org/10.1021/bi300010w | *Biochemistry* 2012, 51, 6266−6288

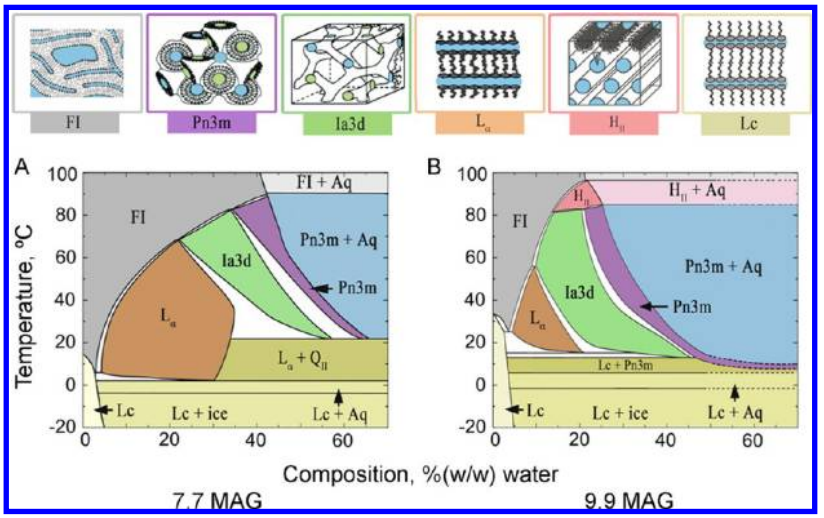

Figure 2. Temperature–composition phase diagrams for (A) 7.7 MAG and (B) 9.9 MAG, two monoacylglycerols that have proven to be particularly useful hosting lipids for the *in meso* crystallization of membrane proteins, complexes, and peptides (Table 1). Cartoon representations of the different solid (Lc), liquid (FI), and liquid crystalline phases (L_α, H_{II}, cubic-Pn3m, cubic-Ia3d) accessed in the temperature and composition range studied are shown along the top of the figure. The phase diagrams were constructed on the basis of small-angle X-ray scattering measurements.[48,133]

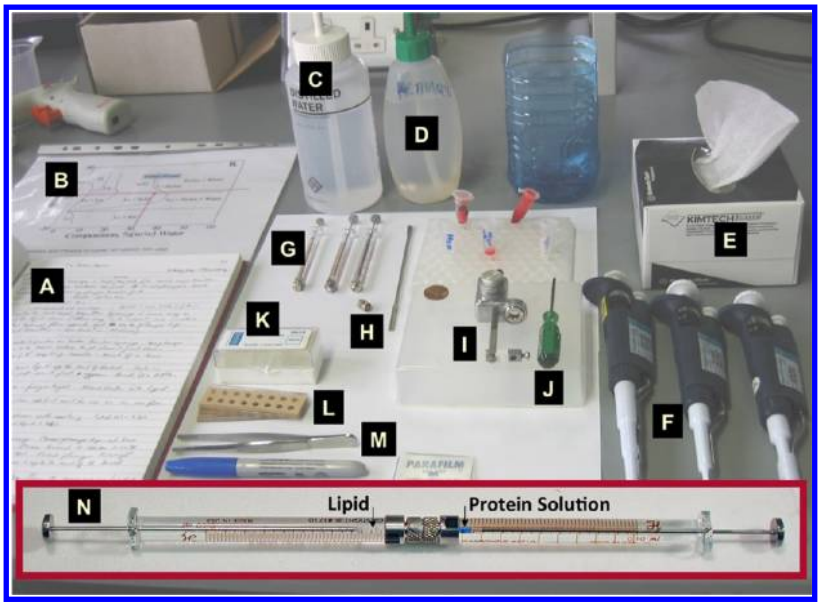

Figure 3. Tools and supplies used to set up *in meso* crystallization trials in manual mode. Full details of the *in meso* method are available in print[45] and in an online video:[46a,46b,46c] (A) laboratory notebook, (B) temperature–composition phase diagram, (C) Milli-Q water, (D) methanol, (E) paper towels, (F) pipeting devices covering volumes in the microliter range, (G) Hamilton syringes (removable needle type, gastight) of varying sizes (10 and 100 μL usually), (H) narrow bore coupler, (I) repeat dispenser, (J) screwdriver, (K) glass slides and coverslips, (L) perforated double-sided tape, (M) tweezers, and (N) coupled syringes loaded with lipid and proteins solution, as indicated.

12, 3, 3, and 4 should be directly accessible to quenching by bromo-MAG, provided the target is reconstituted into the cubic phase bilayer. The extent (>80%) of quenching observed (Figure 7) is consistent with this expectation and supports the view that the targets are reconstituted prior to crystallization.

Some additional evidence that supports a bilayer location derives from the fact that the quenching behavior of gramicidin was sensitive to the acyl chain identity of the accompanying, nonquenching MAG.[59] Because the chains are confined to the bilayer interior, some property(ies) of the bilayer itself changes with the different MAGs. This is sensed by gramicidin presumably only when it is associated with that same lipid bilayer. In so doing, it responds differently to the quenching effect of the brominated lipid, which has a distinct character imprinted on it by the different nonquenching MAGs. One of the properties that changes with MAG identity is bilayer thickness. This, in turn, defines the relative positions of the apolar–polar interface across the membrane that will affect the fluorescence behavior of the tryptophans that sample such an environment.

A final piece of evidence for bilayer location hinges on the logic that gramicidin is so apolar that it is unfavorable for it to reside anywhere else within the confines of the mesophase. SAXS data show that the cubic phase can accommodate gramicidin to a point. Beyond that limit, it triggers a transformation to the H_{II} phase.[59] This presumably reflects a change in the energetics associated with mismatch between the

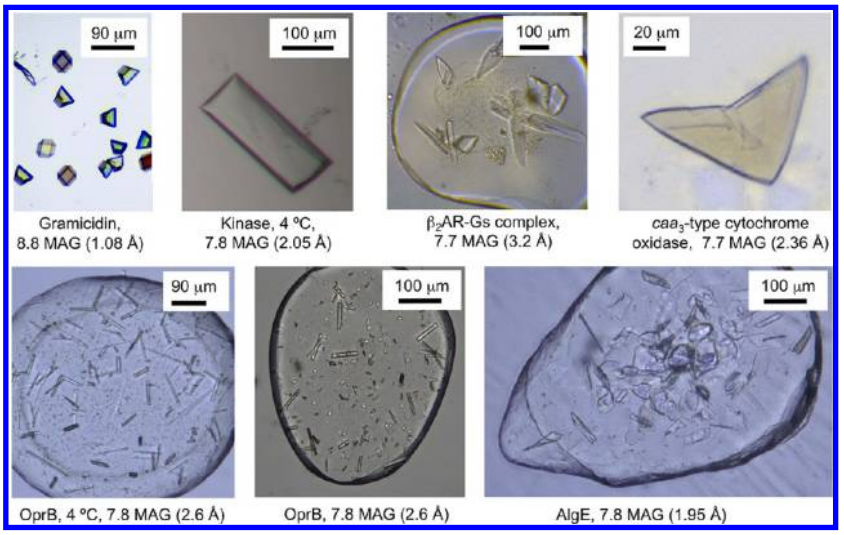

Figure 4. Crystals of membrane proteins in mesophases prepared with different hosting lipids. Examples of proteins and peptides are shown that did not produce crystals or produced crystals that were of lesser diffraction quality in the benchmark lipid, 9.9 MAG (monoolein), compared to the identified MAG. Diffraction quality (parentheses) is identified as is crystal growth temperature if other than 20 °C. Images for the gramicidin and β_2AR−Gs complex are from refs 74 and 12, respectively. In all cases, the protein is colorless but the crystals are clearly visible in the hosting mesophase in wells of the glass sandwich crystallization plate.

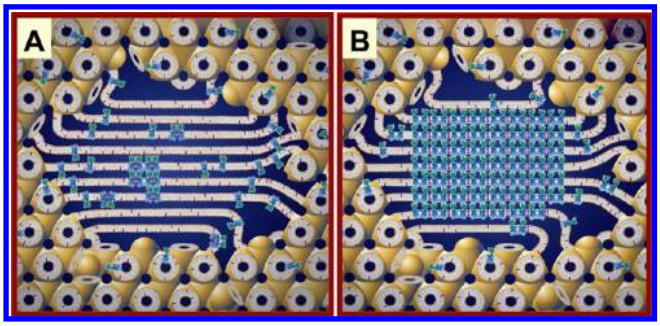

Figure 5. Cartoon representation of the events proposed to take place during the crystallization of an integral membrane protein from the lipidic cubic mesophase. The process begins with the protein reconstituted into the curved bilayer of the "bicontinuous" cubic phase (tan). Added "precipitants" shift the equilibrium away from stability in the cubic membrane. This leads to phase separation wherein protein molecules diffuse from the bicontinuous bilayer reservoir of the cubic phase into a sheetlike or lamellar domain (A) and locally concentrate therein in a process that progresses to nucleation and crystal growth (B). Cocrystallization of the protein with native or additive lipid (cholesterol) is shown in this illustration. As much as possible, the dimensions of the lipid (tan oval with tail), detergent (pink oval with tail), cholesterol (purple), protein (blue and green; β_2-adrenergic receptor−T4 lysozyme fusion; PDB entry 2RH1), bilayer, and aqueous channels (dark blue) have been drawn to scale. The lipid bilayer is ∼40 Å thick.[44] Reproduced from ref 138. Copyright 2011 American Chemical Society.

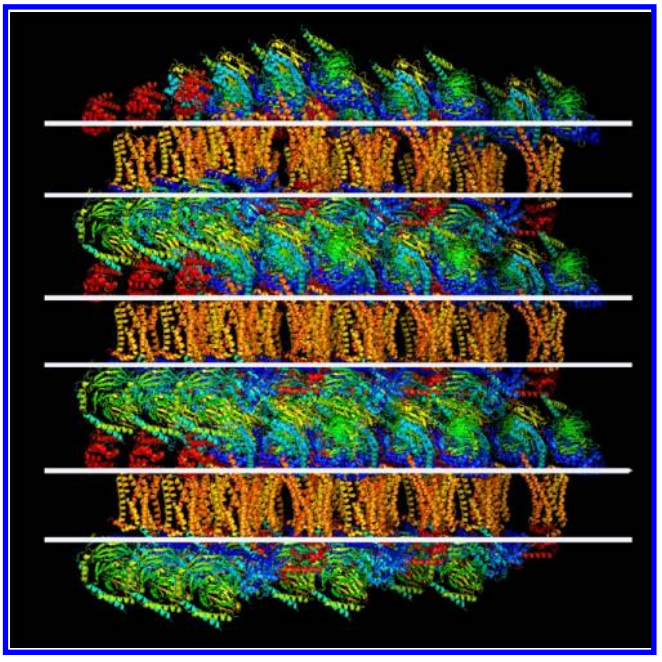

Figure 6. Layered or type I packing is observed in all crystals of membrane proteins produced to date by the *in meso* method. In the case of the β_2-adrenoreceptor−Gs protein complex shown here (PDB entry 3SN6),[12] the transmembrane receptor (tan) drives the layering process by the proposed mechanism outlined in Figure 4. The approximate location of the bilayer supporting the receptor is indicated by the paired horizontal white lines.

peptide and the lipid−water interface, which is a result of a gramicidin that is bilayer-bound.

Conformation. Spectroscopic measurements were taken to examine the conformational state of three membrane proteins and gramicidin reconstituted in the cubic phase. The UV−visible spectra of the BtuB[57] and OpcA[58] preparations in micellar form and *in meso* were, within experimental error, the same regardless of the protein dispersion state. In the case of LHII, a similar observation held, with the exception of a slight change in bacteriochlorophyll absorption in the range of 780−900 nm.[60] Circular dichroism spectra showed that the gross secondary structure of both BtuB[57] and OpcA[58] was insensitive to whether they were in a micellar or a bilayer environment. Together, these data suggest that cubic phase reconstitution does not dramatically alter the conformation of protein targets consistent with the hypothesis.

Functional Activity. It is assumed that proteins reconstituted prior to crystallization retain functionality *in meso*. In the case of BtuB, this was examined by measuring binding of the substrate [cyanocobalamin (CNCbl)] to the protein reconstituted into

dx.doi.org/10.1021/bi300010w | *Biochemistry* 2012, 51, 6266−6288

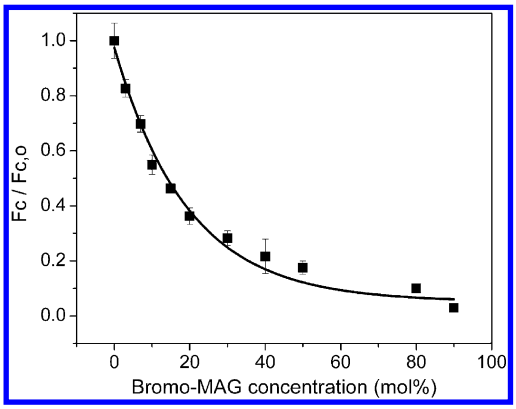

Figure 7. Intrinsic tryptophan fluorescence quenching curve of gramicidin D in the cubic phase of hydrated monoolein. Bromo-MAG is the quenching lipid, and its concentration is expressed as the mole percent in monoolein. Flourescence data were corrected for background fluorescence from buffer and lipid and for the inner filter effect and were normalized to the quencher-free ($F_{c,0}$) value. The quenching profile is consistent with the peptide being reconstituted into the bilayer of the cubic phase. Data were taken from ref 59.

the cubic phase.[57] Protein-free control samples exhibited no binding, whereas test *in meso* BtuB-containing samples showed convincing evidence of substrate uptake. Binding was shown by quenching of intrinsic fluorescence of aromatic residues by CNCbl and by direct ligand binding to be tight with an apparent K_d value of ~1 nM. Similar K_d values have been reported for the native membrane-bound and micellarized form of the protein. Binding of sialic acid to OpcA, measured by fluorescence quenching as with BtuB, was identical *in meso* and in detergent solution.[58] Taken together, the data support the view that these β-barrel proteins reconstitute into the bilayer of the cubic phase in an active form prior to *in meso* crystallization.

Functional activity assays *in meso* have been extended to include membrane protein enzymes.[62] In the case of diacylglycerol kinase (DgkA), a coupled enzyme assay was used (Figure 8). With phosphatidylglycerol phosphate synthase (PgsA), activity was quantified by direct assay. In both cases, the viscous, sticky, and porous nature of the cubic phase was used to advantage in allowing continuous spectrophotometric activity assays to be performed in a high-throughput microplate format. With both enzymes, the cubic mesophase served as a useful and convenient nanoporous membrane mimetic that supported nativelike activity.

Recent studies with the dopamine 2 long (D2L) and histamine 1 (H1) GPCRs indicate ligand binding in the nanomolar range based on radiolabeled assays.[63] In this study, the receptors were reconstituted into the cubic phase by a passive method (see below) and showed significantly enhanced specific binding compared to that of their detergent-solubilized counterpart.

Diffusion. Crystallization, regardless of how it happens, requires transport, i.e., the movement of the crystallant from the bulk medium up and into the face of the crystal. If transport is impeded or does not happen, crystallogenesis will suffer. Under *in meso* conditions, mobility must take place both in the bilayer and in the aqueous channels of the mesophase. When colored proteins, such as bacteriorhodopsin, are used, mobility is noticeable with a simple light microscope. As crystals form, flecks of dark purple appear surrounded by a zone of colorless mesophase, whose distance from the crystal increases with time

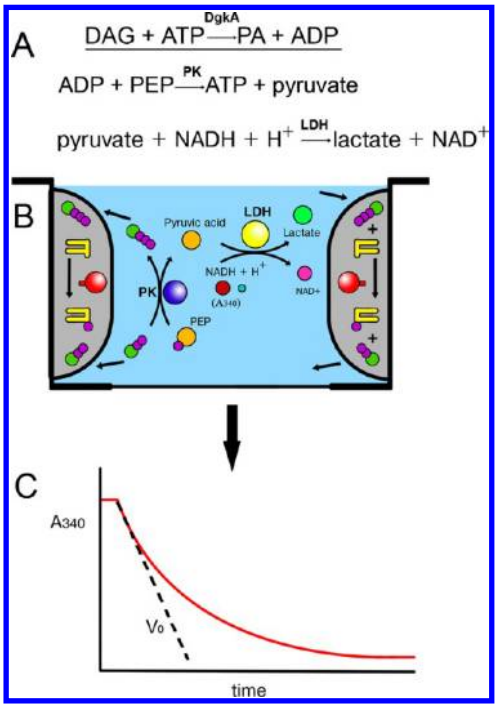

Figure 8. Monitoring the γ-phosphoryl group transfer activity of diacylglycerol kinase (DgkA) reconstituted into the bilayer of the cubic phase by a coupled enzyme assay method (A) in a muliwell plate.[62] Protein-laden mesophase (shaded in gray in panel B) is positioned on the wall of the well where it remains in place throughout the assay as a consequence of its intrinsic viscosity and stickiness. The mesophase is bathed in buffer (blue) containing the water-soluble ingredients of the coupled assay [ATP, ADP, pyruvate, lactate, phosphoenolpyruvate (PEP), NADH/NAD$^+$, pyruvate kinase (PK), and lactate dehydrogenase (LDH)]. The water-soluble substrate, ATP, diffuses into the nanoporous mesophase for use by DgkA in synthesizing phosphatidic acid from diacylglycerol, both of which reside in and are confined to the bilayer of the mesophase. The water-soluble product, ADP, diffuses out of the mesophase into the bathing solution where it is used by the coupled enzyme assay system to regenerate ATP. The coupling process that involves PK and LDH leads to a decrease in the concentration of NADH that, in turn, is monitored continuously in situ in a multiplate reader by a reduction in absorbance at 340 nm of the bathing solution (C). The slope of the progress curve (C) provides a measure of the initial velocity, V_o, as indicated.

and crystal growth. This is evidence that the protein is moving from the mesophase reservoir, presumably in the lipid bilayer, to the crystal. Additional and more quantitative evidence that mobility in the bilayer is required for *in meso* crystallogenesis comes from recent fluorescence recovery after photobleaching measurements performed with labeled bacteriorhodopsin and a GPCR-T4 lysozyme (T4L) fusion.[64] In this case, diffusion and a high fractional recovery of fluorescence in the bleached area correlated with known *in meso* crystallization conditions.

The diffusion of gramicidin, LHII, and a highly lipophilic dye, Sudan Red, has been used to characterize the transport properties of the cubic phase.[60,65] To this end, a bolus of diffusant-loaded cubic phase, the source, was placed in direct contact with a bolus of diffusant-free cubic phase, the sink, at a sharp interface. The transfer of diffusant between the two boluses and subsequent diffusion in the sink were monitored by UV−visible spectroscopy and were shown to occur. In the case of the brightly red colored Sudan Red, transport could be seen with the naked eye.[39] These observations show that the cubic

phase supports transport and, because at least two of these diffusants are highly apolar, that diffusion is most likely taking place within the lipid bilayer. The results also highlight the fusogenic nature of the cubic phase, suggesting that the bilayer of one bolus can become continuous with the bilayer of the other bolus with which it makes contact. This means that the bilayer composition of a given bolus can, within limits, be adjusted at will, which has implications for seeding, cocrystallization, and complex formation by a stepwise approach to *in meso* crystallogenesis.

In the context of *in meso* crystallogenesis, the cubic phase is viewed as a porous molecular sponge consisting of two interpenetrating nanochannels filled with an aqueous medium and coated by a common lipid bilayer. In the preceding paragraphs, it was shown that proteins move within the membrane, a requirement for crystallogenesis. Mobility within the aqueous channels is also a prerequisite for crystal growth, at the very least to allow precipitant components to access the interior of the bolus and to trigger nucleation and crystal growth.

Several studies that support such transport have been performed, and for reasons of experimental simplicity, most were conducted by following the release of water-soluble diffusants from a bolus of preloaded cubic phase.[62,66−68] The studies show that the diffusion rate was dependent on the size of diffusant molecules as expected, given that the channels within the mesophase have a diameter of ∼50 Å. Remarkably, transport was observed[66] with apoferritin, whose size (∼100 Å diameter) far exceeds that of the aqueous channel, suggesting a molecular breathing or peristalsis type of facilitated diffusion.[d] Exquisite control over the rate of movement within the aqueous channels was achieved by adjusting (a) channel dimensions (see the sponge phase below), (b) the partitioning of the diffusant on or into the lipid bilayer, (c) the electrostatic interaction strength, and (d) histidine tag displacement. Thus, although the mesophase channels are small and confined, just 15 water molecules wide, they allow simple and well-behaved transport.

In support of this, ultrafast hydration dynamics studies revealed that the channels include a water core with bulk-like dynamics and orientational relaxation properties consistent with transport.[70] In contrast, the water at the aqueous−bilayer interface is dynamically rigid. The bilayer is surrounded by a hydrogen-bonded network of water with dynamic relaxations intermediate between those of the interfacial and core water. Taken together, these data support the view that the cubic phase behaves as a nanoporous molecular sponge into and out of which water-soluble substances of a wide range of sizes and chemistries can diffuse, which is integral to the *in meso* crystallization model.

The ability of the cubic phase to act as a nanoporous membrane mimetic for integral membrane enzymes also supports the view that facile transport into and out of the aqueous channels of the mesophase does happen.[62] Two lipid-metabolizing enzymes were assayed kinetically on the basis of water-soluble substrates diffusing into and water-soluble products diffusing out of the mesophase bolus in which the enzymes were reconstituted. In one case, the activity measurement was done by a coupled assay; in the other, a direct assay was performed.

Type I Crystal Packing and the Lamellar Phase. The hypothesis posits that the protein migrates from the bulk mesophase reservoir to the face of the crystal by way of a lamellar conduit.[1,43,44] Using a submicrometer-sized X-ray beam, the interface between a growing membrane protein crystal and the bulk cubic phase has been examined with micrometer spatial resolution.[71] Characteristic diffraction from the lamellar phase was observed at the crystal interface, which supports the proposal that the protein uses a lamellar portal on its way from the bulk mesophase up and into the face of the crystal.

There are two reports based on microscopy that address the *in meso* growth of membrane protein crystals by way of a lamellar conduit. The first of these involved freeze-fracture electron microscopic (EM) examinations of acetylcholine receptor−α-bungarotoxin complex microcrystals grown from within a lipid mesophase.[53] EM images showed highly ordered domains of the complex next to lipid lamellae, consistent with the working hypothesis. In the second study, atomic force microscopy was used to demonstrate the existence of a lamellar conduit between the bacteriorhodopsin crystal and the bulk cubic phase.[72]

In meso crystallization is predicted to produce type I crystals (Figures 5 and 6). Here, proteins are arranged in planar sheets that stack one atop the other. Direct protein−protein interactions within the plane of a given layer can be extensive in type I crystals. Type II crystals[2] are commonly encountered when grown by *in surfo* methods. In this case, a torus of detergent coats the protein where it contacted the apolar region of the biomembrane from which it came originally. As a result, direct contact between the apolar midriff of the protein is much less likely in type II crystals, and packing density and diffracting power can be low. To date, all membrane proteins that have been crystallized by the *in meso* method have given rise to type I crystals (Figure 6) (http://www.mpdb.tcd.ie/),[73] consistent with the hypothesis. However, nonlamellar-type packing could be observed at some point with *in meso*-grown crystals. This might occur via a polymorphic transition in the solid state.[44] Presumably, the type I crystal will form first, to be replaced by a more stable polymorph in which the proteins are no longer arranged in distinct lamellae. It is possible, too, that the transition will occur after the protein concentrates locally in the partially ordered lamellar domain (Figure 5) that subsequently produces crystals.[74]

■ TERMINOLOGY

As noted, the cubic phase method is based on the assumption that the protein to be crystallized is initially reconstituted into the lipid bilayer of the cubic phase. However, the phase that feeds the face of the growing crystal is likely to be lamellar, not cubic.[43,44,71] Further, while the monoolein/water phase diagram (Figure 2) upon which the method is based shows that the cubic phase is stable under conditions that approximate those used in crystallization, there are other ingredients in the crystallization mix that can destabilize the cubic phase, locally or even totally converting it to another phase. It is for this reason that we sought to determine the identity of the bulk mesophase(s) present before and during crystal growth. SAXS measurements were used for the purposes of phase identification. For the most part, the prevailing mesophase was found to be of the cubic type. However, this is not always the case, and the phases present vary with the concentration of protein (and detergent) and the identity and concentration of the precipitants used.[75] Thus, we have found that at high concentrations of added protein (bacteriorhodopsin was the test membrane protein), coexisting lamellar (L_α) and cubic

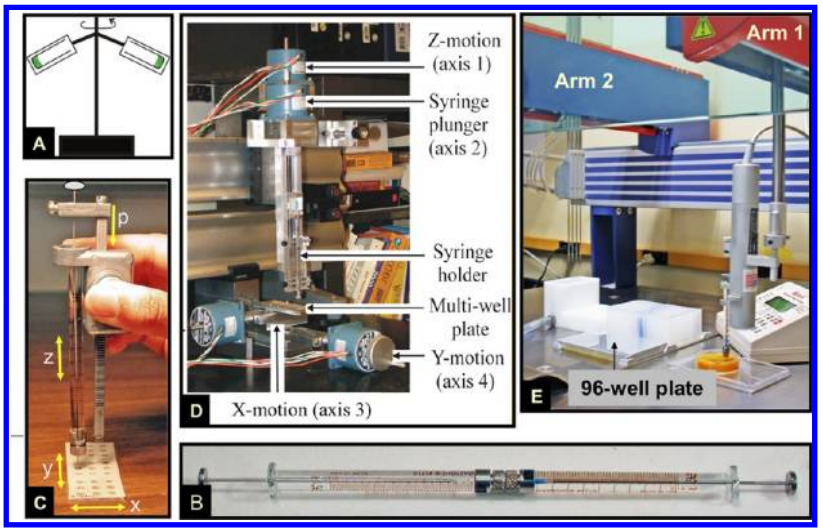

Figure 9. Approaches and equipment used to set up *in meso* crystallization trials since the method was introduced in the mid-1990s. The original method used repeated centrifugation in a fixed angle rotor (A) to effect lipid and protein solution homogenization and cubic phase formation.[38] The coupled syringe mixing device[49] (B) was introduced in 1998 as a more practical and efficient means for generating and dispensing conveniently nanoliter volumes of protein-laden mesophase for use in *in meso* crystallization trials. Manual dispensing of the protein-laden mesophase prepared in the coupled syringe mixing device was greatly facilitated by the repeat dispenser (C).[77] The *x*, *y*, and *z* motions executed in dispensing mesophase manually, as in panel C, inspired the building of a prototype robot consisting of a series of motorized orthogonal translation stages connected to a computer under LabView control (D). The success of the prototype in "automatically" setting up crystallization plates in which membrane protein crystals grew was the proof of concept and enough to secure funding with which to build in-house a custom-designed *in meso* crystallization robot (E).[51] Variations on the original robot shown in panel E are now available commercially.[79−83] The instrument shown in the figure comes equipped with a four-tip liquid handling dispensing arm. An eight-tip version of the instrument is available commercially.

phases form initially. Upon incubation with the Na^+/K^+ phosphate salt "precipitant", the L_α phase converted to the cubic phase such that crystallization took place from a bulk cubic phase medium.[76] In other systems, the cubic phase does not necessarily remain stable throughout the crystal growing period, and it can transform with time to a birefringent or a liquid phase, depending on the precipitant used. Increasingly, the sponge phase is identified as the medium in which crystals grow (see the sponge phase below).

From this discussion, it is apparent that the exclusivity of the cubic phase as the hosting and portal medium is not cast in stone and that other mesophases, or media derived from and reminiscent of them, may play a role. It is for this reason that the less limiting *in meso*, as opposed to the original *in cubo* or lipidic cubic phase (LCP) or more recent lipidic sponge phase (LSP), descriptor is preferred and continues to be used by the authors. An equally accurate and acceptable descriptor is the "lipidic mesophase crystallization" or LMC method.

MINIATURIZATION AND HIGH-THROUGHPUT CRYSTALLIZATION

The protocol described in Experimental Aspects refers to the manual mode of setting up crystallization trials. Accurate and precise delivery of the sticky and viscous protein-laden mesophase in volumes that range from pico- to microliters was made possible by use of an inexpensive repeat dispenser in combination with differently sized microsyringes.[77,78] Smaller volumes mean that the *in meso* method works with miniscule quantities of the target protein. Thus, extensive crystallization screening can be done with just a few micrograms of valuable membrane protein, making the *in meso* method one of the most efficient in terms of required protein, lipid, and precipitant.

The repeat dispenser greatly facilitated the *in meso* method. However, it was still a manual setup with limits to the numbers of trials that any one person could comfortably set up at a sitting. The need to automate the process was obvious. With the assistance of A. Peddi and Y. Zheng, engineers at The Ohio State University (Columbus, OH) where the original work was done, we were able to perform a proof-of-principle robotics exercise employing LabView-controlled motorized translation stages operating and supporting a microsyringe and a crystallization plate. With it, we demonstrated that the viscous mesophase could be dispensed automatically and wells filled in such a way that crystals were eventually produced. This was enough to secure funding for a robot that was custom-designed and built in-house to our specifications (Figure 9).

The *in meso* robot has two arms programmed to move simultaneously over a stationary crystallization plate.[79] One arm dispenses the viscous, protein-laden mesophase, while the other dispenses precipitant. Typical volumes used are 50 nL of mesophase (usually consisting of 20 nL of protein solution and 30 nL of monoolein) and 800 nL of precipitant solution. Custom, 96-well glass sandwich plates that take just 5 min to fill using an eight-tip robot were designed. The robot allows the precise and accurate setting up of *in meso* crystallization trials with very small volumes in high-throughput mode and, if required, under challenging conditions of reduced temperature and controlled lighting. Given the success of the original *in meso* robot, several such instruments, available through commercial vendors,[79−83] are currently in use in laboratories around the world. Variants on the original design, where tip alignment is done automatically and/or where precipitant is handled by disposable tips, are now available commercially.[80,83] Another dispenses 96 precipitant solutions simultaneously providing for very rapid plate setup.[81] These represent important advances simplifying *in meso* crystallogenesis and making the method user-friendly. An online video of how to set up trials robotically is available.[46c]

With the success that the *in meso* method has had, it perhaps is not unexpected to find products appearing on the market in support of this proven crystallogenesis approach. In addition to the *in meso* robots, these include a number of precipitant screen kits, glass and plastic sandwich plates, and a plate that comes complete with lipid-coated wells. The latter are convenient in that they can be used with a liquid-dispensing robot for protein solution delivery first and precipitant postswelling. Variations on this approach have been reported.[63,84,85] It is important to note when using this passive approach that the time required for complete hydration of the lipid and reconstitution prior to precipitant addition will depend on the specifics of the target protein, the composition of the solution in which it is dissolved, the thickness and identity of the hosting lipid, and the temperature. These, in turn, can impact reproducibility. Protracted incubation, with the aim of improving reproducibility, may compromise the protein.

MEMBRANE PROTEIN TARGET ISSUES

General. Although the focus of this article is crystallization, a word about the protein ingredient of the crystal is in order. As noted, suitable starting material is often in short supply. Much effort is currently devoted to increasing the yield of membrane proteins in a crystallizable form. Sources include cellular membranes that the protein calls home. Under the best of circumstances, the membrane will come enriched naturally in the target protein, as in the case of bacteriorhodopsin and the purple membrane. At the other extreme are proteins that are not at all plentiful, and enormous amounts of biomaterials, effort, and time must be devoted to procuring mere microgram quantities. The GPCRs and the cystic fibrosis transmembrane conductance regulator (CFTR) are such proteins.[86,87] Overexpression in a host organism can be used to boost yield. However, it is not unusual for the membrane protein to compromise or kill the host cell when overproduced. One way around this is to bypass the membrane altogether and to express the protein in vivo as an insoluble cytoplasmic inclusion body[88,89] or in vitro in a variety of dispersed states.[90] This then requires that the protein be solubilized, often in concentrated solutions of urea or guanidine hydrochloride, with or without detergent, followed by a refolding step in the presence of a detergent as a prelude to crystallogenesis. As an alternative, we have proposed using solubilized inclusion bodies for direct *in meso* crystallization.[68] The logic is as follows. The protein, dissolved in a concentrated denaturant (urea, for example) solution, is used to form the cubic phase. Upon incubation with excess refolding buffer, the urea rushes out of the porous mesophase and the protein begins to refold. Because it is essentially trapped in the narrow aqueous confines of the cubic phase, the protein is only in ångströms from the lipid bilayer and spontaneously reconstitutes into it. The protein-laden mesophase can then be used directly for *in meso* crystallogenesis. The fact that such proteins never encounter a natural membrane raises questions regarding the fidelity of the structure so determined. With OmpG[91,92] and a recent case involving the biofilm alginate transporting AlgE from *Pseudomonas aeruginosa*, virtually identical structures were obtained with protein isolated from membranes (J. Tan, D. Li, D. Aragao, V. Pye, and M. Caffrey, unpublished observations) and protein refolded from inclusion bodies.[93]

When cloning is used, advantage can be taken of the ability to engineer in sequences (affinity tags) and/or fusion proteins that facilitate purification and crystallization, as well as amino acid analogues, such as selenomethionine for phasing purposes. Fusions that include the green fluorescent protein (GFP) or its homologues can be used for convenient and high-throughput screening of expression, purification, and indeed crystallization.[94,95] For this to work, however, the GFP tag needs to be cytoplasmic and the tagged protein should be properly folded. Protocols and vectors are available to ensure a cytoplasmic localization.[96] Including in the recombinant protein a protease site for optional removal of the tag or fusion protein prior to crystallization is the norm. The recombinant approach also affords the opportunity to modify the target should the native protein prove to be refractory to crystallization. Such modifications include N- and/or C-terminal as well as internal sequence trimming or extension and removal of undesired post-translational modification sites. Exploring the crystallizability of thermostabilized mutants and of homologues of the target protein from other organisms is a proven strategy with membrane proteins.[94,95,97−99] Often, in cases where the perceived business end of the molecule is not in the membrane, the membrane-anchoring part of the protein is removed. This reduces the task to crystallizing a soluble polypeptide whose structure, it is hoped, will faithfully represent that of the intact membrane-associated protein. Neuraminidase is one such example.[100−103]

This same "pruning" approach can be taken as a last resort in pursuit of at least some structural information about the more complex, multidomain membrane proteins, such as the CFTR. Domains that are not likely to be buried in the membrane can be expressed separately or excised from the intact protein and used in crystallization trials. However, functional insights gleaned from structural information derived using this "divide and conquer" approach must be evaluated with caution. A bonus is that should diffraction-quality crystals of the intact protein be obtained subsequently, the determined soluble domain structure might be used for phasing by molecular replacement.

As with soluble proteins, every effort must be made to ensure that the membrane protein used in crystallization trials is stable and of the highest possible biochemical and conformational purity and homogeneity. Assessments of purity based on electrophoresis, size exclusion chromatography, single-particle electron microscopy, analytical ultracentrifugation, and light and X-ray scattering can be used to advantage here. More recently, mass spectrometry (MS) has emerged as an important alternative and/or supplement to the more traditional analytical techniques given that it offers picomole sensitivity, high mass accuracy, high-throughput capability, and speed, all at a reasonable cost.[104−106] Furthermore, mass spectrometers are ubiquitous, and most institutions now provide MS facilities and support on a routine service basis.

With regard to target purity, a word of caution is in order in that a membrane protein can be "too pure" and, as a result, does not yield crystals of the desired quality. This happens when the protein is purified to such an extent that it is stripped of structurally important lipids and/or cofactors. Thus, working with a less pure preparation is worth trying. Alternatively, lipids can be included in the purification buffers or added back to the protein preparation prior to crystallization trials. There are several examples in the literature where the right amount and type of added lipid proved to be critical to the production of structure-quality crystals.[107−110] In the case of the GPCRs, cholesteryl hemisuccinate (CHS) is commonly included in the buffers used for purification and the hosting mesophase for

crystallization is spiked with cholesterol to this same end.[7−10,12−20,22,25,26,111−114]

GPCRs. In addition to the *in meso* crystallization technology, novel protein-related complementary strategies have proven to be crucial to the recent spate of high-resolution crystal structures of GPCRs, in the inactive and active conformations. These involve increasing the crystal contact surface area, conformational homogeneity, and thermostability of purified receptors.

Crystal contact enhancement involved the replacement of the third intracellular loop with a modified T4 lysozyme. Extensive mutagenesis and biochemical studies were performed to show that the flexible third intracellular loop of the β_2-adrenergic receptor (β_2AR) could be replaced with the relatively stable, ordered, and crystallization-prone T4L.[22] The resulting β_2AR−T4L fusion protein displayed similar pharmacological properties but enhanced stability compared to the wild-type receptor. Further, the fusion construct trafficked to the cell surface and could be crystallized by the *in meso* and bicelle methods.[7,22] This highly effective T4L fusion approach has since been applied to a number of other GPCRs whose crystal structures have been determined by the *in meso* method.[8−10,13−18,20,111−114] A recent variation on this approach leaves the third intracellular loop intact and fuses a thermostabilized apo-cytochrome b_{562}RIL from *E. coli* to the truncated N-terminus of the receptor to promote receptor stability and *in meso* crystallogenesis.[19] Separately, a rhodopsin-inspired single-amino acid (3.41 according to Ballesteros−Weinstein numbering[115]) mutation in the third transmembrane helix that significantly enhances the functional expression and thermal stability of class A GPCRs is now standard practice.[116] To produce a structure of the fully active, agonist-bound form of β_2AR, high-affinity nanobodies (camelid antibodies) were generated that, in association with the receptor or the receptor−Gs complex, promoted active state conformational homogeneity, stability of the G protein complex, and crystal contacts that facilitated *in meso* crytallogenesis.[12,25] Receptor stability can be optimized using a convenient, high-throughput fluorescence assay that measures cysteine accessibility upon denaturation of the purified receptor.[117] An alternative approach uses ligand binding assays to membranes isolated from recombinant *E. coli* in what is termed "conformational thermostabilization".[98,118−122] To date, this method that employs scanning and additive mutagenesis has been used for GPCR structure determination only by the *in surfo* method of crystal production.[11,123−125]

SAMPLES WITH LOW PROTEIN CONCENTRATIONS

The driving force for nucleation is stronger the more supersaturated the system. Thus, a common strategy in crystallization is to work at the highest possible protein concentration to favor nucleation and to lower its concentration subsequently to just above the solubility limit for slow, orderly growth of a few high-quality crystals. It is likely that the same principles apply to crystallization *in meso* where initially, the highest possible protein concentration should be used in support of nucleation. There are at least two issues that must be considered in this context that apply to membrane proteins. First, most membrane proteins are prepared and purified in combination with detergents. Thus, the detergent is carried along with the protein into the crystallization mix. It follows then that as the protein concentration increases, the detergent concentration will increase in parallel. This may work against crystallization because high levels of detergent destabilize the hosting mesophase.[76,126] Of course, the sensitivity to added detergent will depend, among other things, on the identities of the hosting lipid and detergent. Completely removing the detergent before folding the protein into the crystallization mix is usually not an option because it is commonly required to keep the protein soluble as a mixed micelle. One alternative is to reduce the detergent load to an acceptable level before combining the protein with the hosting lipid. This can be done with BioBeads[76,127] or by eluting the protein in a highly concentrated form from an affinity column. Using detergents with low critical micelle concentrations, such as lauryl maltose neopentyl glycol (MNG-DDM), is also worth investigating.

The second issue has to do with increasing the concentration of the protein in the lipid bilayer of the cubic phase to facilitate nucleation. Two approaches can be tried that are quite different but that achieve the same end. The first exploits the water-carrying capacity of the cubic phase, a property that varies with lipid identity (see Figure 2).[128−133] Thus, the reconstituted protein will be more concentrated in the bilayer of the cubic phase prepared with a lipid with a high water-carrying capacity than with a less hydrating lipid. The second approach involves sequential reconstitutions where the protein concentration in the bilayer increases with each round.[e]

LIMITS TO MESOPHASE COMPATIBILITY

Protein Solution Components. As mentioned above, what happens during *in meso* crystallization is intimately tied to lipid mesophase behavior.[44] The working hypothesis for how nucleation comes about begins with the protein reconstituting into the continuous bilayer of the cubic phase (Figure 2). Precipitant is added, which triggers local formation of a lamellar phase into which the protein preferentially partitions and concentrates in a process that leads to nucleation and crystal growth (Figure 5). As noted, experimental evidence in support of aspects of this model has been reported.

Experience, built up over several years working with the *in meso* method, suggests that the mesophase behavior observed during the course of the crystallization process mimics that of the relevant MAG (where the default MAG is monoolein)/water system (Figure 2). The implication therefore is that the protein solution has a minimal effect on the phase behavior of the hosting lipidic mesophase into which the protein is reconstituted. That solution, along with the target protein, typically includes lipid, detergent, buffers, and salt at a minimum. Other components such as glycerol, sulfhydryl reagents, denaturants, etc., are not uncommon. Each of these can have an impact on phase behavior and, by extension, on the outcome of a crystallization trial. In the interests of learning about component compatibility, the sensitivity of the monoolein/water cubic phase system to their inclusion has been evaluated. Our findings indicate that the default cubic mesophase is remarkably resilient and retains its phase identity in the presence of a vast array of different additives. These include glycerolipids, cholesterol, free fatty acids, detergents, denaturants, glycerol, and sulfhydryl reagents, among others.[43,60,66−68,75,76,126,134] Of course, for each there is a concentration beyond which the cubic phase is no longer stable. In most cases, these limits have been identified.

Occasionally, the concentration of a protein solution component is not known exactly. Detergent is a case in point. This poses a problem because if there is too much detergent the bulk lamellar phase may form and this will not

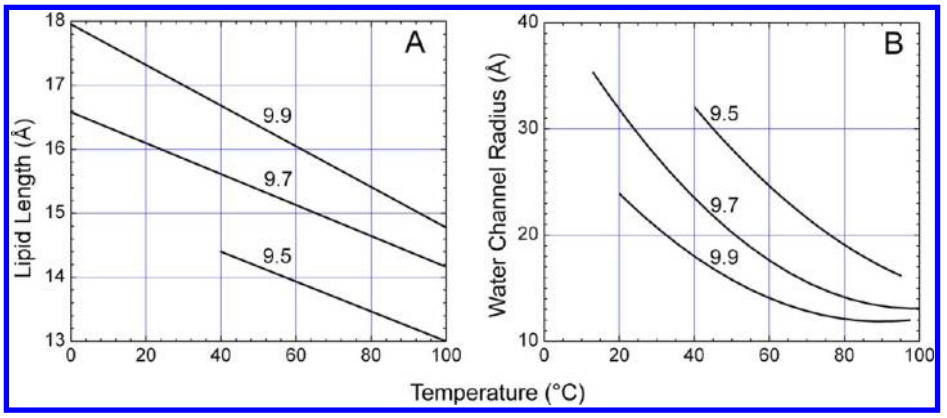

Figure 10. Temperature-induced changes in the lipid and aqueous channel dimensions of the cubic phase. Temperature dependence of the lipid length in the cubic phase (A) and of fully hydrated, cubic *Pn3m* phase water channel radius (B) for three monoacylglycerols. Lipid identity is reported in the *N.T* notation. Data are from refs 128, 130, and 131.

support crystallization.[76,126] It may also be that a new detergent is being used, whose compatibility with the cubic phase is not known. In this case, a small amount of the buffer used to solubilize the protein or the protein solution itself can be used to prepare the mesophase. The physical texture (high viscosity), the appearance between crossed polarizers, or the SAXS behavior of the mesophase will indicate which phase has been accessed. If, for example, it is a lamellar phase that forms suggesting too much detergent, then another purification step at which its concentration in the final protein solution is reduced may be enough to solve the problem. We have encountered situations with bacteriorhodopsin in which the particular preparation ended up having an excess of detergent. The mesophase first formed was lamellar, but when it was used in combination with certain precipitants, a transition back to the cubic phase was induced, which went on to support crystal growth.[76]

Crystallization Screen Solution. As noted, *in meso* crystallization relies upon a bicontinuous mesophase that acts as a reservoir to feed protein into nucleation sites and for crystal growth (Figure 2). The crystallization screening process requires that chemical space be interrogated over wide limits. In the screening process therefore, the protein-laden mesophase is exposed to precipitant solutions that encompass hundreds, perhaps even thousands, of different chemical compositions. Screen solution components include buffers that cover a wide buffer type and pH range, polymers, salts, small organics, detergents, apolar solvents, amphiphiles, etc., all at different concentrations. Each component can potentially destabilize the mesophase. In a separate study using SAXS, we examined the compatibility of the reference monoolein/water cubic phase with various commonly used precipitant screen solutions.[75] What we found was hardly surprising. Compatibility was temperature-dependent, and the usual suspects, including organic solvents, destroyed the cubic phase, rendering these screen solutions effectively useless. A goal of the study was to design screens that were mesophase friendly. However, that goal was never pursued; instead, we have opted for the convenience of commercial screen kits mindful of the fact that certain conditions are not relevant. As a result, certain kits are simply not used because they contain too few conditions that are compatible with the cubic phase. Others are used in diluted form. For example, PACT premier (MD1-36, Molecular Dimensions) is used at 50−65% of full strength.

SPONGE PHASE

During the course of mesophase compatibility studies, we noticed that particular screen components caused the cubic phase to "swell" and, under certain conditions, to form what is termed the sponge phase. The latter evolves from the cubic phase as a result of the "spongifying" component lowering the extent of bilayer interfacial curvature, thereby allowing the mesophase to imbibe more lyotrope (aqueous solution). This is revealed in the SAXS pattern where the lattice parameter of the cubic phase rises. Eventually, the mesophase looses order and the low-angle diffraction pattern becomes diffuse. Fortunately, the sponge phase retains its bicontinuity and, as a result, can support *in meso* crystallogenesis.[44,60,135] One advantage of the sponge phase is that its aqueous channels are dilated. Thus, proteins with large extramembrane domains should be accommodated in and amenable to crystallogenesis from the sponge phase. Further, the reduced interfacial curvature is likely to facilitate more rapid and long-range diffusion within the lipid bilayer. Because net movement of protein from the bulk mesophase reservoir to the nucleation and growth sites is a requirement for crystallization, this effect alone should contribute to improved crystallization. Interestingly, many of the proteins that have yielded to the *in meso* method have been crystallized under conditions that favor sponge phase formation (http://www.mpdb.tcd.ie).[73]

Reflecting the utility of the sponge phase for *in meso* crystallogenesis, a number of commercial screening kits now include spongifiers such as polyethylene glycol, Jeffamine, butanediol, 2-methyl-2,4-pentanediol (MPD), and pentaerythritol propoxylate (PPO), among others. Some of these provide a preformed sponge phase to which the protein solution is added directly. We continue to use the original method that involves an active protein reconstitution step with pure lipid where the entire crystallization screen space is available for sampling.

LIPID RATIONAL DESIGN

Low-Temperature Crystallogenesis. The MS&FB Group has devoted considerable time and effort to establishing the structure−function rules for rationally designing lipids with specific end uses.[1,136−138] One such application concerned the development of a host lipid for use in *in meso* crystallogenesis at low temperatures. Certain proteins are labile and require handling in the cold. The problem with the *in meso* method, in

the default mode at least, is that it relies on monoolein as the hosting lipid. The cubic phase formed by monoolein is not stable below ~17 °C (Figure 2B),[48] and performing crystallization trials in a cold room at 4−6 °C is risky. For this low-temperature application therefore, a *cis*-monounsaturated monoacylglycerol, 7.9 MAG, was designed, using the rules described above. The target MAG was synthesized and purified in-house and its phase behavior mapped out using SAXS.[136] As designed, it produced the cubic phase stable in the range from 6 to 85 °C. 7.9 MAG has been used in the crystallization of a number of membrane proteins by the MS&FB Group.

The word "risky" was used in the previous paragraph when referring to low-temperature crystallization with monoolein as the hosting lipid. This reflects the fact that it is possible to do successful *in meso* work with monoolein at 4 °C provided the system undercools. Fortunately, the cubic phase is noted for this capacity,[48,131] and we perform successful crystallization trials regularly with monoolein in the 4−17 °C range. As expected, under these metastable conditions, occasionally the mesophase converts to the bulk lamellar crystalline (Lc) or solid phase, which is no use as far as crystallogenesis is concerned.[f]

Tailoring Mesophase Microstructure To Match the Target Protein. With regard to *in meso* crystallization, it is important to appreciate that the microstructure of the phase can change with, among other things, temperature, sample composition (hydration is one example), and lipid identity.[48,140] By microstructure is meant the lattice parameter of the phase and how it is constituted. Thus, for example, the lamellar phase consists of planar sheets of lipid bilayers each separated by a layer of water (Figure 2). As the temperature, composition, and lipid identity change, the thickness of the lipid bilayer as well as that of the water layer can change. The same holds true for the other mesophases, including the bicontinuous phases (Figure 10).

Hydrated monoolein in the cubic phase at 20 °C may provide a suitable matrix in which to grow membrane protein crystals. However, decreasing the temperature to 4 °C, while preserving the cubic phase as a result of metastability, will cause the lattice parameter to change and, along with it, the dimensions of the lipid bilayer (Figure 10A) and the water channels (Figure 10B) of the cubic phase.[48,131] It is possible that such changes may no longer ensure retention of protein activity or support crystal growth for a host of reasons. By the same token, it may well provide an even more stabilizing and a better crystal-growing environment. We are currently quantifying the effects that lipid and water compartment sizes of the cubic phase have on the stability and crystallizability of several membrane proteins.

Reference has just been made to the sensitivity of phase microstructure to lipid identity. Support for this statement is based on X-ray diffraction measurements performed on the cubic phase of a homologous series of MAGs (Figure 10).[1] The data show expected behavior in that as the chain length decreases so too does the thickness of the lipid layer that creates the apolar fabric of the cubic phase, when evaluated at a single temperature (Figure 10A). Less intuitive perhaps is the finding that the aqueous channel diameter becomes smaller as the chain length increases (Figure 10B). This is consistent with a "flattening" and an attenuating curvature at the polar−apolar interface with the shorter chain lipids.

While lipid identity can be used to tailor phase microstructure, it is possible that the desired microstructure might not be accessible with a single lipid species in the temperature range of interest. In this case, it is possible to fine-tune by using mixtures of MAGs with different acyl chain characteristics where the mole ratio is adjusted to set microstructure at the desired intermediate value.[1]

It is apparent from the data just presented that it is possible to engineer the microstructure of the mesophase over relatively wide limits by manipulating temperature and/or lipid identity and composition. However, it is also important to note that the two metrics of the cubic phase, the polar and apolar compartment dimensions, are not independently adjustable and indeed are tightly coupled, as indicated in Figure 10. Nonetheless, this feature of tunability is an important tool that is available to the crystallographer in search of a suitable lipid matrix in which to grow crystals. Thus, proteins with transmembrane and extramembrane domains that come in a variety of sizes can be accommodated as can those that originate from native membranes with different hydrophobic thicknesses.[141]

Proteins and Complexes with Large Membrane Footprints and Large Extramembrane Domains. In what follows, two recent examples of rational lipid design for use in crystallizing targets with large footprints in the plane of the membrane and/or extensive extramembrane domains are described. The first refers to cytochrome caa_3 oxidase from *T. thermophilus*. This terminal oxidase is a large 120 kDa heterotrimeric protein with 23 transmembrane helices and a cytochrome *c*-like domain as a C-terminal extension to one of its subunits. Extensive crystallization trials by traditional vapor diffusion methods failed to produce structure-grade crystals. The *in meso* method was considered as an appropriate alternative. At the time the study was undertaken, *in meso* crystallization had generated crystals and a structure of a protein, LHII, whose bulk in the plane of the membrane resembled that expected for caa_3. Initial *in meso* trials with the default lipid, 9.9 MAG or monoolein, failed to produce useful crystals. With the anticipation of the likelihood that 9.9 MAG would not suit every membrane protein, the lipid synthesis program of the MS&FB Group provided alternative MAGs with which to screen for crystallogenesis. The first of these tested was 7.7 MAG, which has an acyl chain 14 carbon atoms long and a *cis* double bond between carbons 7 and 8. 7.7 MAG had been shown to form a cubic mesophase with a thinner, less highly curved bilayer and with enlarged aqueous channels.[133] A thinner bilayer was considered desirable for use with caa_3 because it more suitably complemented the hydrophobic thickness predicted for related cytochrome oxidases of known structure. Additionally, the larger aqueous channels provided by 7.7 MAG were attractive in the context of caa_3 with its added extramembrane bulk in the form of a cupredoxin and a tethered cytochrome *c*-like domain. As expected, 7.7 MAG produced crystals; upon optimization, they provided a structure at 2.36 Å.[137]

The second example is the β_2-adrenergic receptor−Gs protein complex. Earlier work had shown that the free receptor produced structures to high resolution in the default lipid, 9.9 MAG, using the *in meso* method. However, efforts to grow structure-grade crystals of the receptor as a complex with its cognate Gs protein in monoolein failed. The Gs protein is itself a large heterotrimeric complex with a molecular mass of ~80 kDa. It binds to the exposed intracellular surface of the receptor and adds considerable extramembrane bulk to the target. In this particular instance, the Gs protein had bound to it a camelid

antibody or nanobody (15 kDa) and T4L (19 kDa) was fused to the N-terminus of the receptor. Both contributed additional extramembrane heft to the complex. Given that the cubic phase prepared with monoolein alone has aqueous channels in which the water-soluble domains that are only 50 Å in diameter must reside,[131] failure to crystallize in monoolein did not come as a surprise. 7.7 MAG, with its significantly larger aqueous channels, was immediately identified as a suitable alternative hosting lipid, and with some limited optimizations, it generated diffraction-quality crystals and a structure of the complex.[12] Interestingly, the precipitant used for the production of final crystals included PEG 400, a known spongifier, and crystals were harvested from what appeared to be a sponge phase. It seems likely therefore that the short chain MAG and the spongifier worked hand in hand to generate a bicontinuous medium that accommodated unrestricted diffusion and that facilitated crystallization of the complex with its extensive extramembrane domain. Future *in meso* crystallization trials with targets of this sort will undoubtedly benefit from the use of short chain MAGs in concert with sponge phase-inducing precipitants. Commercial crystallization kits that include such materials are likely forthcoming. It is important to note that in all of the aforementioned GPCR work, the hosting MAG was doped with cholesterol (see the following section).

LIPID SCREENING

Host Lipid. The original lipid used for *in meso* crystallogenesis was monoolein. It was recognized from the outset that this one lipid may not work with all target membrane proteins. The rationale was that these come from a variety of native membranes that differ in lipid composition, bilayer thickness, surface charge and packing density, fluidity and polarity profile, intrinsic curvature, etc. Thus, having a range of MAGs that differed in acyl chain characteristics available for screening was deemed important. Using principles of rational design, a number of suitable MAGs were identified with the requirement that they form the inverse cubic phase at or close to 20 °C under conditions of full hydration. Several lipids meeting these specifications have been synthesized and characterized in house. They now constitute an invaluable hosting lipid screen in the MS&FB Group. With a number of membrane proteins, including β-barrels, α-helical proteins and complexes, and an integral peptide antibiotic, crystals have been grown by the *in meso* method using these alternative hosting MAGs.[12,74,133,136,138] In a number of instances, monoolein failed to produce crystals or the crystals it did produce were not of diffraction quality. It was only when MAGs from the hosting lipid screen were used that structure-grade crystals were obtained (Figure 4). Some of these novel MAGs are available commercially.[142]

Additive Lipid. Early on in the development of the *in meso* method, it was recognized that monoolein, as the lipid used to create the hosting mesophase, is not a typical membrane lipid.[1,134] The sense was that it might be recognized as foreign by certain target proteins and trigger a destabilization reaction. One solution considered was to employ a naturally occurring membrane lipid that forms the requisite cubic phase under crystallization conditions. Unfortunately, none was available. An alternative was to use the default MAG, monoolein, as the hosting lipid and to supplement it with typical membrane lipids with a goal of creating a more nativelike environment. Accordingly, the carrying capacity of the monoolein cubic phase for a number of different lipids was established using SAXS.[134] This amounted to ~20 mol % in the case of phosphatidylcholine, phosphatidylethanolamine, and cholesterol with smaller amounts of phosphatidylserine and cardiolipin being accommodated. With time, other lipids will need to be included in *in meso* crystallization trials. The carrying capacity of the cubic phase for such lipids can be evaluated by SAXS, as noted,[134] or less quantitatively but more simply and immediately by evaluating the texture and optical clarity and by polarized light microscopy.[45] The strategy of using additive lipids has proven to be particularly useful with GPCR targets where cholesterol augmentation of the cubic phase was critical to the production of diffraction-quality crystals and was seen in the final determined structure (Figure 11).[7−10,12−20,22,25,26,111−114] Given the success of this approach, pre-prepared lipid mixtures for use in *in meso* crystallization trials are available commercially.[143]

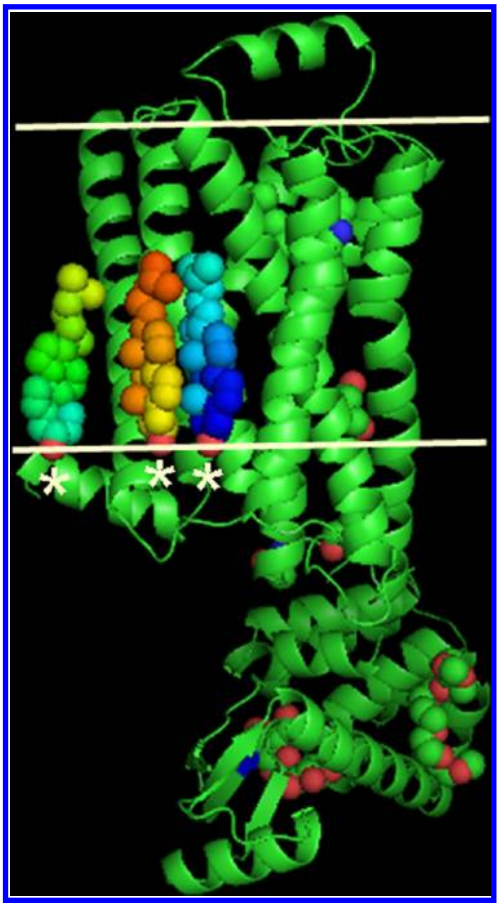

Figure 11. Structure of the β_2-adrenoreceptor determined with crystals grown by the *in meso* method using monoolein doped with cholesterol as an additive lipid. Cholesterol molecules (space filling model, asterisks) are part of the crystal structure. White horizontal lines mark the approximate location of the membrane−aqueous interface with respect to the receptor (green model, PDB entry 2RH1).

CRYSTAL STRUCTURES

The *in meso* method accounts for 103 records in the Protein Data Bank (http://www.pdb.org) that relate to integral membrane proteins and peptides (Tables 1 and 2 and http://www.mpdb.tcd.ie).[73] This corresponds to ~10% of published membrane protein structures and represents at least eight distinct classes of membrane proteins (Figure 12). With

dx.doi.org/10.1021/bi300010w | *Biochemistry* 2012, 51, 6266−6288

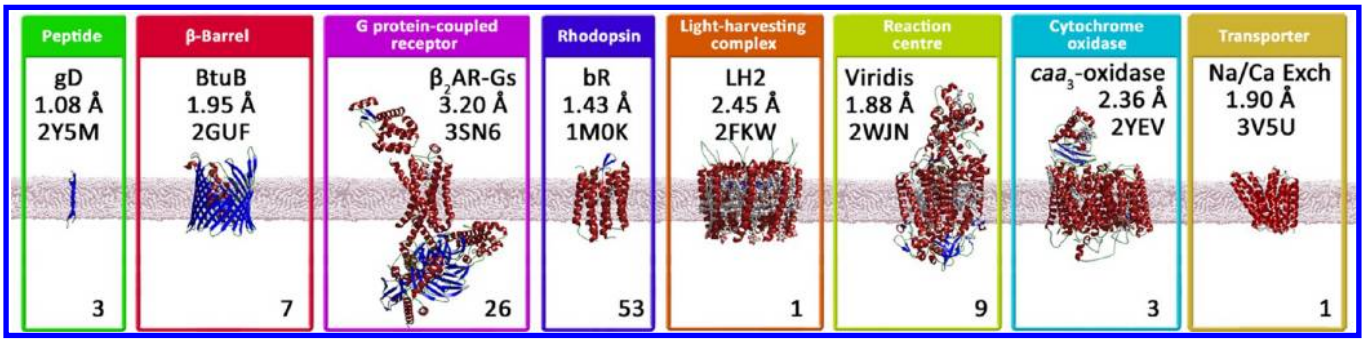

Figure 12. Gallery of membrane protein structures determined using crystals grown by the lipidic cubic phase or *in meso* method. A single representative structure within a membrane protein class is shown along with the diffraction resolution and PDB accession code. The figure at the bottom of each panel refers to the number of record entries in the PDB for that particular membrane protein class. Thus, within the peptide class there are three records for gramicidin D at different resolutions. Within the β-barrel class, there are seven entries, one each for BtuB, OpcA, Intimin, and Invasin and three for OmpF. Within the G protein-coupled receptor class, there are 26 records: one for the β_2-adrenoreceptor−Gs complex, seven for the β_2-adrenorecptor, three for the A_{2a}-adenosine receptor, five for the CXCR4 receptor, two for the sphingosine 1-phosphate subtype 1 receptor, and one each for the D3 dopamine receptor, the H1 histamine receptor, the M2 muscarinic receptor, the M3 muscarinic receptor, the δ-opioid receptor, the κ-opioid receptor, the μ-opioid receptor, and the nociceptin receptor. Within the non-GPCR rhodopsin class, there are 53 records: 38 for bacteriorhodopsin, three for halorhodopsin, six for sensory rhodopsin II, three for the sensory rhodopsin II−transducer complex, and one each for sensory rhodopsin from *Nostoc* sp. PCC 7120 and rhodopin from *A. acetabulum*. Within the light-harvesting complex class, there is a single entry for LHII. Within the photosynthetic reaction center class, there are five and four entries for the reaction centers from *B. viridis* and *R. sphaeroides*, respectivly. Within the cytochrome oxidase class, there are two entries for ba_3 and one for caa_3. Within the exchanger group, there is a single entry for the Na^+-Ca^{2+} exchanger. As of July 2012, the total count for *in meso* structures in the PDB is 103.

successes that include bacterial and eukaryotic rhodopsins, the sensory rhodopsin II−transducer complex, LHII, photosynthetic reaction centers, cytochrome oxidases, β-barrels, GPCRs, a GPCR−Gs complex, an exchanger, and an integral membrane peptide, the method has a convincing record of versatility and range. Each of these membrane protein types represents families the members of which are also candidates for *in meso* crystallogenesis. The GPCR family is the latest case in point; it has approximately 800 distinct GPCRs and ∼20 cognate G proteins encoded by the human genome alone. The *in meso* method therefore, in combination with the necessary protein engineering and receptor stabilization strategies, is poised to contribute to the generation of GPCR and receptor−G protein complex structures on an "industrialized" scale. Evidence in support of this statement is the recent spate of GPCR structures courtesy, in part, of *in meso* crystallogenesis (Table 2). This past year alone has witnessed at least eight such deposited structures in the PDB. It is with some confidence therefore that we can look forward to successes with other membrane protein families.

The further development of the *in meso* crystallogenesis approach is an important goal for the MS&FB Group. Recently, this has focused on examining the utility of the method with small membrane proteins. A separate analysis performed using a model cubic phase under somewhat limiting conditions indicated that suitable targets would need to include a minimum of five transmembrane helices.[144] Our experience with the sponge phase variant of the cubic phase suggested otherwise. Accordingly, the utility of the method with a "mini-protein", the penta-decapeptide antibiotic, linear gramicidin, was examined. It worked remarkably well, providing a structure for the intertwined conformation of the antibiotic with a resolution of 1.08 Å.[74,145] Regardless of the chain length of the hosting MAG used, the antibiotic grew crystals in the intertwined conformation. A word of caution is in order here. The physiological relevance of the latter, intertwined form has been questioned, and the issue was considered in detail by Hoefer et al.[74] Several mechanistic proposals for how this, as opposed to the head-to-head, conformation crystallized *in meso* have been presented.[74,145] Regardless, the result obtained with linear gramicidin highlights the utility of the method with proteins having small transmembrane domains that abound in nature.[146]

■ MEMBRANE PROTEIN DATA BANK

Details regarding the structure and function of integral, anchored, and peripheral membrane proteins are available online in a convenient and searchable database, the Membrane Protein Data Bank (MPDB, http://www.mpdb.tcd.ie).[73] Records in the MPDB are obtained from the PDB. However, the former limits itself to entries for membrane proteins. Statistical analyses of the contents of the database can be performed conveniently and viewed directly online. Examples include the detergents or pH or temperature used for membrane protein structure work, number of structures published annually by method, etc.

■ PROSPECTS

The *in meso* method burst on the scene a decade and a half ago. It was received with great anticipation for what it would deliver; perhaps it was to be the panacea. However, output in the early years was limited to naturally abundant, bacterial α-helical proteins bedecked with stabilizing and highly colored prosthetic groups (http://www.mpdb.tcd.ie).[73] The perceived restricted range, coupled with the challenges associated with handling the sticky and viscous cubic mesophase, meant that subsequent interest in the method waned. This was countered to some degree with the introduction of the *in meso* robot, a growing understanding for how the method worked at a molecular level, and a continued demonstration of the method's general applicability. However, interest in the method has rocketed of late with the success it has had in the GPCR field (Table 2).[7−10,12−20,22,25,26,111−114]

Improvements are needed of course if the method is to become routine. Critically, the specialized materials and supplies upon which the method relies must be made more

generally available, and the method itself must be made user-friendly. New and improved *in meso* robots available on the market are tackling the user-friendliness issue. Workshops that involve hands-on demonstrations contribute to making the method more accessible. The author has been active in this area for several years now with recent workshops in Ireland,[147] Mexico,[148] Hawaii,[149] Australia,[150] and China.[151] In the past year alone, more than 200 students were trained in the practicalities and finer elements of *in meso* crystallogenesis and related topics at various locations worldwide. Online video demonstrations covering practical aspects of the method are available.[46a,46b,46c]

Developments are needed in the area of crystal identification. Optical clarity is of the highest quality with the glass sandwich plates currently in use, and this provides for ready detection of colorless, micrometer-sized crystals in normal light and between crossed polarizers. Detection by UV fluorescence is particularly powerful and convenient for tryptophan-containing proteins. Fluorescence labeling[52,53] is also a route worth considering for the sensitive detection of early hits. Second-order nonlinear optical imaging of chiral crystals (SONICC) is a novel approach introduced by G. Simpson. It has been shown to sensitively and selectively detect membrane protein crystals growing *in meso*.[152]

Recovering crystals from the mesophase for data collection is a nontrivial undertaking.[45,46b] This is especially true when harvesting is done directly from glass sandwich plates. Typically, a glass cutter is used to open the well and to expose the mesophase. Teasing out and harvesting the crystal for immediate cryo-cooling is most conveniently done with a cryo-loop. This is a slow, painstaking, and cumbersome process especially if it must be done in a cold room and/or in subdued light. This whole area of harvesting calls out for innovation to include automation.

Collection of data at the synchrotron is not exactly straightforward either. Given that *in meso*-grown crystals tend to be small, a mini-synchrotron X-ray beam is required. Oftentimes, the crystal of interest is hidden from view in a bolus of mesophase on the cryo-loop. This means that locating the crystal and centring it requires rounds of diffraction rastering with a beam progressively smaller in size.[153,154] This same approach is used to advantage in finding the best diffracting part of a crystal. Locating crystals and centering based on X-ray fluorescence from heavy atoms in the sample is in development (D. Aragao, M. Becker, D. Li, M. Hilgart, J. Lyons, D. Yoder, S. Stepanov, R. Fischetti, and M. Caffrey, unpublished observations). Effective and efficient rastering is recognized now as an important feature of the latest MX beamlines at synchrotron facilities worldwide, and steady improvements in the rastering process are being made. In situ screening and data collection as well as dynamic focusing for improved signal to noise are other areas under investigation. The wherewithal to screen and to collect data efficiently over the Internet and without the need for travel to the synchrotron is eagerly anticipated.

The X-ray free electron laser (XFEL) is a tantalizing new technology for MX of membrane proteins.[155,156] Here, femtosecond pulses at 10^{12-13} X-rays/pulse strike a flowing stream or extruded bolus micrometers in diameter that ports equally sized or smaller crystals into and through the X-ray beam. Each pulse, delivered at 120 Hz, has enough energy to raise the temperature of the striken crystal to beyond that of the sun's core. But because the pulse is of such short duration, diffraction from the "native state" can occur, and be collected subsequently, before the crystal is converted to a plasma. Both the cubic and sponge mesophases[157] are being investigated as media for transporting crystals into the XFEL beam with the prospect of being able to collect structure-quality diffraction data using material that might otherwise be abandoned as microcrystalline or mistakenly identified as precipitated protein. The distinct possibility exists that such microcrystals are superior to their more voluminous counterparts with respect to diffraction quality, requiring shorter times to grow and less material to produce a structure. Additional XFEL sources dedicated to such measurements will be needed.

The structures determined using *in meso*-grown crystals have, until very recently,[158−160] relied on molecular replacement for phasing.[g] Increasingly, experimental phasing will be required. In our hands, with poorly diffracting crystals, this is proving to be a challenge. Several targets have been tackled using selenomethionine labeling and prelabeling, cocrystallization, and soaking with heavy atoms with only limited success. Problems derive in part from a low anomalous signal to noise due to a combination of background low- and wide-angle scatter from adhering mesophase and the need to work with small and sometimes poorly diffracting, radiation-sensitive crystals. As often as not, data must be collected in angular wedges on different parts of a single crystal or on multiple crystals, and merging data satisfactorily is a challenge. This part of the *in meso* pipeline is in need of work.

Finally, the method should begin to be used with really small and with large proteins and complexes. The sponge phase,[60] with its open aqueous channels and flatter bilayer, should prove to be particularly useful in this regard. Using it in combination with novel hosting and additive lipid screens[74,134,138] will go a long way toward producing crystals and ultimately high-resolution structures in which interactions that are integral to human health are revealed.

AUTHOR INFORMATION

Corresponding Author

*Membrane Structural and Functional Biology Group, School of Medicine and School of Biochemistry and Immunology, Trinity College Dublin, Dublin, Ireland. Telephone: 353-1-896-4253. Fax: 353-1-896-4253. E-mail: martin.caffrey@tcd.ie.

Funding

This work was supported in part by grants from Science Foundation Ireland (07/IN.1/B1836), FP7 COST Action CM0902, Marie Curie Actions (PIEF-GA-2009-254103), and the National Institutes of Health (GM75915, P50GM073210, and U54GM094599).

Notes

The authors declare no competing financial interest.

ACKNOWLEDGMENTS

There are many who contributed to this work, and most are from the MS&FB Group, both past and present members. To all we extend our warmest thanks and appreciation.

ABBREVIATIONS

CNCbl, cyanocobalamin; CHS, cholesteryl hemisuccinate; EM, electron microscopy; FI, fluid isotropic phase; GFP, green fluorescent protein; GPCR, G protein-coupled receptor; H_{II}, inverted hexagonal phase; L_{α}, lamellar liquid crystal phase; L_{c}, lamellar crystal phase; LCP, lipidic cubic phase; LDH, lactate

dehydrogenase; LHII, light-harvesting complex II; LMC, lipidic mesophase crystallization; LSP, lipidic sponge phase; MAG, monoacylglycerol; MNG, maltose neopentyl glycol; MPD, 2-methyl-2,4-pentanediol; MPDB, Membrane Protein Data Bank; MS, mass spectrometry; MS&FB, Membrane Structural and Functional Biology; MX, macromolecular X-ray crystallography; PDB, Protein Data Bank; PEP, phosphoenolpyruvate; PK, pyruvate kinase; PPO, pentaerythritol propoxylate; SAXS, small-angle X-ray scattering; SONICC, second-order nonlinear optical imaging of chiral crystals; T4L, T4 lysozyme; UV, ultraviolet; XFEL, X-ray free electron laser.

■ ADDITIONAL NOTES

[a]The bulk of the *in meso* crystallogenesis performed to date employs MAGs containing *cis*-monounsaturated fatty acids. A shorthand system for describing the chemical constitution of these MAGs makes use of the *N.T* notation introduced previously.[47] This is based on a rather simplistic view of the MAG molecule as an object consisting of a head, a neck, and a tail with the latter two joined by a trunk. The head is the glycerol headgroup. It is in ester linkage with the neck corresponding to that part of the acyl chain extending from its carboxyl carbon to the first carbon of the olefin. The trunk is the *cis*-double bond. The tail extends from the second carbon of the olefin to the chain's methyl terminus. In the *N.T* MAG notation, *N* and *T* correspond to the number of carbon atoms in the neck and tail, respectively. The total number of carbon atoms in the chain is the sum of *N* and *T*. Thus, 11.7 MAG represents monovaccenin, a MAG with a fatty acyl chain 18 carbon atoms long in which the *cis*-double bond resides between carbon atoms 11 and 12. It is an olefinic isomer of 9.9 MAG also known as monoolein.

[b]Should too much protein solution be employed, the mesophase would become cloudy and opaque. If possible, this should be avoided as it can create problems in recognizing small crystals commonly encountered as initial hits. If the cloudy, two-phase system does form, it can still be used for the successful crystallization provided the mesophase is of the bicontinuous (nonbirefringent) type.[45]

[c]For comparison, crystals of the β_2AR–Gs complex 0.25 mm long formed *in meso* in 2–3 days.[12] This corresponds to an average growth rate of ~5 μm/h.

[d]This is consistent with the observation that transducin, a large heterotrimeric G protein, can diffuse from solution into a rhodopsin-loaded cubic phase sample and form a functional complex.[69]

[e]The membrane protein preferentially partitions from the aqueous solution into the bilayer of the cubic phase. If the reconstitution step is repeated using a single mesophase bolus and with a series of solutions of protein at low concentrations, the protein load in the mesophase will increase with each reconstitution, leaving excess aqueous solution depleted of protein. This protein-depleted solution is usually removed before the next round of reconstitution commences.

[f]Sugar-phytane lipids form the fully hydrated cubic phase in the 10–70 °C range.[139] These may well find application for *in meso* crystallization at reduced temperatures. In our hands, we have found these lipids difficult to handle. They require very robust mixing, especially below 50 °C.

[g]The recent successes in using experimental phasing for structure determination have occurred with channelrhodopsin from *C. reinhardtii* (PDB entry 3UG9; mercury-MAD), the Na^+-Ca^{2+} exchanger from *M. jannaschii* (PDB entry 3V5U; samarium-SAD), β-barrels from *E. coli* (PDB entry 4E1S; selenomethionine-SAD), and *Y. pseudotuberculosis* (PDB entry 4E1T; selenomethionine-SAD) and with a membrane kinase from *E. coli* (D. Li, J. Lyons, V. Pye, D. Aragao, and M. Caffrey, in preparation; selenomethionine-SAD).

■ REFERENCES

(1) Caffrey, M. (2003) Membrane protein crystallization. *J. Struct. Biol. 142*, 108–132.

(2) Michel, H. (1983) Crystallization of membrane-proteins. *Trends Biochem. Sci. 8*, 56–59.

(3) Chen, Y. J., Pornillos, O., Lieu, S., Ma, C., Chen, A. P., and Chang, G. (2007) X-ray structure of EmrE supports dual topology model. *Proc. Natl. Acad. Sci. U.S.A. 104*, 18999–19004.

(4) Wada, T., Shimono, K., Kikukawa, T., Hato, M., Shinya, N., Kim, S. Y., Kimura-Someya, T., Shirouzu, M., Tamogami, J., Miyauchi, S., Jung, K. H., Kamo, N., and Yokoyama, S. (2011) Crystal structure of the eukaryotic light-driven proton-pumping rhodopsin, *Acetabularia* rhodopsin II, from marine alga. *J. Mol. Biol. 411*, 986–998.

(5) Lahiri, S., Brehs, M., Olschewski, D., and Becker, C. F. W. (2011) Total chemical synthesis of an integral membrane enzyme: Diacylglycerol kinase from *Escherichia coli*. *Angew. Chem., Int. Ed. 50*, 3988–3992.

(6) Deisenhofer, J., and Michel, H. (1989) The photosynthetic reaction center from the purple bacterium *Rhodopseudomonas viridis*. *EMBO J. 8*, 2149–2170.

(7) Cherezov, V., Rosenbaum, D. M., Hanson, M. A., Rasmussen, S. G. F., Thian, F. S., Kobilka, T. S., Choi, H. J., Kuhn, P., Weis, W. I., Kobilka, B. K., and Stevens, R. C. (2007) High-resolution crystal structure of an engineered human β2-adrenergic G protein-coupled receptor. *Science 318*, 1258–1265.

(8) Jaakola, V. P., Griffith, M. T., Hanson, M. A., Cherezov, V., Chien, E. Y. T., Lane, J. R., IJzerman, A. P., and Stevens, R. C. (2008) The 2.6 angstrom crystal structure of a human A2A adenosine receptor bound to an antagonist. *Science 322*, 1211–1217.

(9) Chien, E. Y. T., Liu, W., Zhao, Q. A., Katritch, V., Han, G. W., Hanson, M. A., Shi, L., Newman, A. H., Javitch, J. A., Cherezov, V., and Stevens, R. C. (2010) Structure of the human dopamine D3 receptor in complex with a D2/D3 selective antagonist. *Science 330*, 1091–1095.

(10) Wu, B. L., Chien, E. Y. T., Mol, C. D., Fenalti, G., Liu, W., Katritch, V., Abagyan, R., Brooun, A., Wells, P., Bi, F. C., Hamel, D. J., Kuhn, P., Handel, T. M., Cherezov, V., and Stevens, R. C. (2010) Structures of the CXCR4 chemokine GPCR with small-molecule and cyclic peptide antagonists. *Science 330*, 1066–1071.

(11) Lebon, G., Warne, T., Edwards, P. C., Bennett, K., Langmead, C. J., Leslie, A. G., and Tate, C. G. (2011) Agonist-bound adenosine A2A receptor structures reveal common features of GPCR activation. *Nature 474*, 521–525.

(12) Rasmussen, S. G. F., DeVree, B. T., Zou, Y. Z., Kruse, A. C., Chung, K. Y., Kobilka, T. S., Thian, F. S., Chae, P. S., Pardon, E., Calinski, D., Mathiesen, J. M., Shah, S. T. A., Lyons, J. A., Caffrey, M., Gellman, S. H., Steyaert, J., Skiniotis, G., Weis, W. I., Sunahara, R. K., and Kobilka, B. K. (2011) Crystal structure of the β2 adrenergic receptor-Gs protein complex. *Nature 477*, 549–555.

(13) Shimamura, T., Shiroishi, M., Weyand, S., Tsujimoto, H., Winter, G., Katritch, V., Abagyan, R., Cherezov, V., Liu, W., Han, G. W., Kobayashi, T., Stevens, R. C., and Iwata, S. (2011) Structure of the human histamine H-1 receptor complex with doxepin. *Nature 475*, 65–70.

(14) Granier, S., Manglik, A., Kruse, A. C., Kobilka, T. S., Thian, F. S., Weis, W. I., and Kobilka, B. K. (2012) Structure of the δ-opioid receptor bound to naltrindole. *Nature 485*, 400–404.

(15) Haga, K., Kruse, A. C., Asada, H., Yurugi-Kobayashi, T., Shiroishi, M., Zhang, C., Weis, W. I., Okada, T., Kobilka, B. K., Haga, T., and Kobayashi, T. (2012) Structure of the human M2 muscarinic acetylcholine receptor bound to an antagonist. *Nature 482*, 547–551.

(16) Hanson, M. A., Roth, C. B., Jo, E., Griffith, M. T., Scott, F. L., Reinhart, G., Desale, H., Clemons, B., Cahalan, S. M., Schuerer, S. C., Sanna, M. G., Han, G. W., Kuhn, P., Rosen, H., and Stevens, R. C. (2012) Crystal structure of a lipid G protein-coupled receptor. *Science 335*, 851−855.
(17) Kruse, A. C., Hu, J., Pan, A. C., Arlow, D. H., Rosenbaum, D. M., Rosemond, E., Green, H. F., Liu, T., Chae, P. S., Dror, R. O., Shaw, D. E., Weis, W. I., Wess, J., and Kobilka, B. K. (2012) Structure and dynamics of the M3 muscarinic acetylcholine receptor. *Nature 482*, 552−556.
(18) Manglik, A., Kruse, A. C., Kobilka, T. S., Thian, F. S., Mathiesen, J. M., Sunahara, R. K., Pardo, L., Weis, W. I., Kobilka, B. K., and Granier, S. (2012) Crystal structure of the μ-opioid receptor bound to a morphinan antagonist. *Nature 485*, 321−326.
(19) Thompson, A. A., Liu, W., Chun, E., Katritch, V., Wu, H., Vardy, E., Huang, X. P., Trapella, C., Guerrini, R., Calo, G., Roth, B. L., Cherezov, V., and Stevens, R. C. (2012) Structure of the nociceptin/orphanin FQ receptor in complex with a peptide mimetic. *Nature 485*, 395−399.
(20) Wu, H., Wacker, D., Mileni, M., Katritch, V., Han, G. W., Vardy, E., Liu, W., Thompson, A. A., Huang, X. P., Carroll, F. I., Mascarella, S. W., Westkaemper, R. B., Mosier, P. D., Roth, B. L., Cherezov, V., and Stevens, R. C. (2012) Structure of the human κ-opioid receptor in complex with JDTiC. *Nature 485*, 327−332.
(21) Prive, G. G., and Kaback, H. R. (1996) Engineering the lac permease for purification and crystallization. *J. Bioenerg. Biomembr. 28*, 29−34.
(22) Rosenbaum, D. M., Cherezov, V., Hanson, M. A., Rasmussen, S. G. F., Thian, F. S., Kobilka, T. S., Choi, H. J., Yao, X. J., Weis, W. I., Stevens, R. C., and Kobilka, B. K. (2007) GPCR engineering yields high-resolution structural insights into β2-adrenergic receptor function. *Science 318*, 1266−1273.
(23) Chun, E., Thompson, A. A., Liu, W., Roth, C. B., Griffith, M. T., Katritch, V., Kunken, J., Xu, F., Cherezov, V., Hanson, M. A., and Stevens, R. C. (2012) Fusion partner toolchest for the stabilization and crystallization of G protein-coupled receptors. *Structure 20*, 967−976.
(24) Hunte, C., and Michel, H. (2002) Crystallisation of membrane proteins mediated by antibody fragments. *Curr. Opin. Struct. Biol. 12*, 503−508.
(25) Rasmussen, S. G. F., Choi, H. J., Fung, J. J., Pardon, E., Casarosa, P., Chae, P. S., DeVree, B. T., Rosenbaum, D. M., Thian, F. S., Kobilka, T. S., Schnapp, A., Konetzki, I., Sunahara, R. K., Gellman, S. H., Pautsch, A., Steyaert, J., Weis, W. I., and Kobilka, B. K. (2011) Structure of a nanobody-stabilized active state of the β2 adrenoceptor. *Nature 469*, 175−180.
(26) Rasmussen, S. G. F., Choi, H. J., Rosenbaum, D. M., Kobilka, T. S., Thian, F. S., Edwards, P. C., Burghammer, M., Ratnala, V. R. P., Sanishvili, R., Fischetti, R. F., Schertler, G. F. X., Weis, W. I., and Kobilka, B. K. (2007) Crystal structure of the human β2 adrenergic G protein-coupled receptor. *Nature 450*, 383−387.
(27) Steyaert, J., and Kobilka, B. K. (2011) Nanobody stabilization of G protein-coupled receptor conformational states. *Curr. Opin. Struct. Biol. 21*, 567−572.
(28) Sennhauser, G., and Grutter, M. G. (2008) Chaperone-assisted crystallography with DARPins. *Structure 16*, 1443−1453.
(29) Ostermeier, C., Iwata, S., Ludwig, B., and Michel, H. (1995) Fv fragment mediated crystallization of the membrane-protein bacterial cytochrome *c* oxidase. *Nat. Struct. Biol. 2*, 842−846.
(30) Lee, S. Y., Lee, A., Chen, J., and MacKinnon, R. (2005) Structure of the KvAP voltage-dependent K^+ channel and its dependence on the lipid membrane. *Proc. Natl. Acad. Sci. U.S.A. 102*, 15441−15446.
(31) Jiang, Y., Ruta, V., Chen, J., Lee, A., and MacKinnon, R. (2003) The principle of gating charge movement in a voltage-dependent K^+ channel. *Nature 423*, 42−48.
(32) Jiang, Y., Lee, A., Chen, J., Ruta, V., Cadene, M., Chait, B. T., and MacKinnon, R. (2003) X-ray structure of a voltage-dependent K^+ channel. *Nature 423*, 33−41.
(33) Dutzler, R., Campbell, E. B., and MacKinnon, R. (2003) Gating the selectivity filter in ClC chloride channels. *Science 300*, 108−112.
(34) Zhou, Y., Morais-Cabral, J. H., Kaufman, A., and MacKinnon, R. (2001) Chemistry of ion coordination and hydration revealed by a K^+ channel-Fab complex at 2.0 Å resolution. *Nature 414*, 43−48.
(35) Uysal, S., Vasquez, V., Tereshko, V., Esaki, K., Fellouse, F. A., Sidhu, S. S., Koide, S., Perozo, E., and Kossiakoff, A. (2009) Crystal structure of full-length KcsA in its closed conformation. *Proc. Natl. Acad. Sci. U.S.A. 106*, 6644−6649.
(36) Krishnamurthy, H., and Gouaux, E. (2012) X-ray structures of LeuT in substrate-free outward-open and apo inward-open states. *Nature 481*, 469−474.
(37) Hino, T., Arakawa, T., Iwanari, H., Yurugi-Kobayashi, T., Ikeda-Suno, C., Nakada-Nakura, Y., Kusano-Arai, O., Weyand, S., Shimamura, T., Nomura, N., Cameron, A. D., Kobayashi, T., Hamakubo, T., Iwata, S., and Murata, T. (2012) G-protein-coupled receptor inactivation by an allosteric inverse-agonist antibody. *Nature 482*, 237−240.
(38) Landau, E. M., and Rosenbusch, J. P. (1996) Lipidic cubic phases: A novel concept for the crystallization of membrane proteins. *Proc. Natl. Acad. Sci. U.S.A. 93*, 14532−14535.
(39) Caffrey, M. (2009) Crystallizing membrane proteins for structure determination: Use of lipidic mesophases. *Annu. Rev. Biophys. 38*, 29−51.
(40) Caffrey, M. (2011) Crystallizing membrane proteins for structure-function studies using lipidic mesophases. *Biochem. Soc. Trans. 39*, 725−732.
(41) Faham, S., and Bowie, J. U. (2002) Bicelle crystallization a new method for crystallizing membrane proteins yields a monomeric bacteriorhodopsin structure. *J. Mol. Biol. 316*, 1−6.
(42) Takeda, K., Sato, H., Hino, T., Kono, M., Fukuda, K., Sakurai, I., Okada, T., and Kouyama, T. (1998) A novel three-dimensional crystal of bacteriorhodopsin obtained by successive fusion of the vesicular assemblies. *J. Mol. Biol. 283*, 463−474.
(43) Caffrey, M. (2000) A lipid's eye view of membrane protein crystallization in mesophases. *Curr. Opin. Struct. Biol. 10*, 486−497.
(44) Caffrey, M. (2008) On the mechanism of membrane protein crystallization in lipidic mesophases. *Cryst. Growth Des. 8*, 4244−4254.
(45) Caffrey, M., and Cherezov, V. (2009) Crystallizing membrane proteins using lipidic mesophases. *Nat. Protoc. 4*, 706−731.
(46) (a) Caffrey, M., and Porter, C. (2010) Crystallizing membrane proteins for structure determination using lipidic mesophases. *J. Vis. Exp.*, e1712. (b) Li, D., Boland, C., Aragao, D., Walsh, K., and Caffrey, M. (2012) Harvesting and cryo-cooling crystals of membrane proteins grown in lipidic mesophases for structure determination by macromolecular crystallography. *J. Vis. Exp.*, e4001. (c) Li, D., Boland, C., Walsh, K., and Caffrey, M. (2012) Use of a robot for high-throughput crystallization of membrane proteins in lipidic mesophases. *J. Vis. Exp.*, e4000.
(47) Misquitta, Y., and Caffrey, M. (2001) Rational design of lipid molecular structure: A case study involving the c19:1c10 mono-acylglycerol. *Biophys. J. 81*, 1047−1058.
(48) Qiu, H., and Caffrey, M. (2000) The phase diagram of the monoolein/water system: Metastability and equilibrium aspects. *Biomaterials 21*, 223−234.
(49) Chen, A. H., Hummel, B., Qiu, H., and Caffrey, M. (1998) A simple mechanical mixer for small viscous lipid-containing samples. *Chem. Phys. Lipids 95*, 11−21.
(50) Cherezov, V., and Caffrey, M. (2003) Nano-volume plates with excellent optical properties for fast, inexpensive crystallization screening of membrane proteins. *J. Appl. Crystallogr. 36*, 1372−1377.
(51) Cherezov, V., Peddi, A., Muthusubramaniam, L., Zheng, Y. F., and Caffrey, M. (2004) A robotic system for crystallizing membrane and soluble proteins in lipidic mesophases. *Acta Crystallogr. D60*, 1795−1807.
(52) Forsythe, E., Achari, A., and Pusey, M. L. (2006) Trace fluorescent labeling for high-throughput crystallography. *Acta Crystallogr. D62*, 339−346.

(53) Paas, Y., Cartaud, J., Recouvreur, M., Grailhe, R., Dufresne, V., Pebay-Peyroula, E., Landau, E. M., and Changeux, J. P. (2003) Electron microscopic evidence for nucleation and growth of 3D acetylcholine receptor microcrystals in structured lipid-detergent matrices. *Proc. Natl. Acad. Sci. U.S.A. 100*, 11309−11314.
(54) Nollert, P., Qiu, H., Caffrey, M., Rosenbusch, J. P., and Landau, E. M. (2001) Molecular mechanism for the crystallization of bacteriorhodopsin in lipidic cubic phases. *FEBS Lett. 504*, 179−186.
(55) Khelashvili, G., Mondal, S., Caffrey, M., and Weinstein, H. (2012) Quantitative comparison of GPCR interactions with the lipid bilayer of the cubic and lamellar mesophases. *Biophys. J. 102*, 467a−468a.
(56) McPherson, A. (1999) *Crystallization of biological macromolecules*, Cold Spring Harbor Laboratory Press, Plainview, NY.
(57) Cherezov, V., Yamashita, E., Liu, W., Zhalnina, M., Cramer, W. A., and Caffrey, M. (2006) In meso structure of the cobalamin transporter, BtuB, at 1.95 angstrom resolution. *J. Mol. Biol. 364*, 716−734.
(58) Cherezov, V., Liu, W., Derrick, J. P., Luan, B., Aksimentiev, A., Katritch, V., and Caffrey, M. (2008) In meso crystal structure and docking simulations suggest an alternative proteoglycan binding site in the OpcA outer membrane adhesin. *Proteins: Struct., Funct., Bioinf. 71*, 24−34.
(59) Liu, W., and Caffrey, M. (2005) Gramicidin structure and disposition in highly curved membranes. *J. Struct. Biol. 150*, 23−40.
(60) Cherezov, V., Clogston, J., Papiz, M. Z., and Caffrey, M. (2006) Room to move: Crystallizing membrane proteins in swollen lipidic mesophases. *J. Mol. Biol. 357*, 1605−1618.
(61) Hochkoeppler, A., Landau, E. M., Venturoli, G., Zannoni, D., Feick, R., and Luisi, P. L. (1995) Photochemistry of a photosynthetic reaction-center immobilized in lipidic cubic phases. *Biotechnol. Bioeng. 46*, 93−98.
(62) Li, D., and Caffrey, M. (2011) Lipid cubic phase as a membrane mimetic for integral membrane protein enzymes. *Proc. Natl. Acad. Sci. U.S.A. 108*, 8639−8644.
(63) Darmanin, C., Conn, C. E., Newman, J., Mulet, X., Seabrook, S. A., Liang, Y. L., Hawley, A., Kirby, N., Varghese, J. N., and Drummond, C. J. (2012) High-throughput production and structural characterization of libraries of self-assembly lipidic cubic phase materials. *ACS Comb. Sci. 14*, 247−252.
(64) Cherezov, V., Liu, J., Griffith, M., Hanson, M. A., and Stevens, R. C. (2008) LCP-FRAP assay for pre-screening membrane proteins for in meso crystallization. *Cryst. Growth Des. 8*, 4307−4315.
(65) Clogston, J. (2005) Applications of the lipidic cubic phase: From controlled release and uptake to in meso crystallization of membrane proteins. Ph.D. Thesis, The Ohio State University, Columbus, OH.
(66) Clogston, J., and Caffrey, M. (2005) Controlling release from the lipidic cubic phase. Amino acids, peptides, proteins and nucleic acids. *J. Controlled Release 107*, 97−111.
(67) Clogston, J., Craciun, G., Hart, D. J., and Caffrey, M. (2005) Controlling release from the lipidic cubic phase by selective alkylation. *J. Controlled Release 102*, 441−461.
(68) Liu, W., and Caffrey, M. (2006) Interactions of tryptophan, tryptophan peptides, and tryptophan alkyl esters at curved membrane interfaces. *Biochemistry 45*, 11713−11726.
(69) Navarro, J., Landau, E. M., and Fahmy, K. (2002) Receptor-dependent G-protein activation in lipidic cubic phase. *Biopolymers 67*, 167−177.
(70) Kim, J., Lu, W. Y., Qiu, W. H., Wang, L. J., Caffrey, M., and Zhong, D. P. (2006) Ultrafast hydration dynamics in the lipidic cubic phase: Discrete water structures in nanochannels. *J. Phys. Chem. B 110*, 21994−22000.
(71) Cherezov, V., and Caffrey, M. (2007) Membrane protein crystallization in lipidic mesophases. A mechanism study using X-ray microdiffraction. *Faraday Discuss. 136*, 195−212.
(72) Qutub, Y., Reviakine, I., Maxwell, C., Navarro, J., Landau, E. M., and Vekilov, P. G. (2004) Crystallization of transmembrane proteins in cubo: Mechanisms of crystal growth and defect formation. *J. Mol. Biol. 343*, 1243−1254.
(73) Raman, P., Cherezov, V., and Caffrey, M. (2006) The membrane protein data bank. *Cell. Mol. Life Sci. 63*, 36−51. www.mpdb.tcd.ie.
(74) Hofer, N., Aragao, D., Lyons, J. A., and Caffrey, M. (2011) Membrane protein crystallization in lipidic mesophases. Hosting lipid effects on the crystallization and structure of a transmembrane peptide. *Cryst. Growth Des. 11*, 1182−1192.
(75) Cherezov, V., Fersi, H., and Caffrey, M. (2001) Crystallization screens: Compatibility with the lipidic cubic phase for in meso crystallization of membrane proteins. *Biophys. J. 81*, 225−242.
(76) Misquitta, Y., and Caffrey, M. (2003) Detergents destabilize the cubic phase of monoolein: Implications for membrane protein crystallization. *Biophys. J. 85*, 3084−3096.
(77) Cherezov, V., and Caffrey, M. (2005) A simple and inexpensive nanoliter-volume dispenser for highly viscous materials used in membrane protein crystallization. *J. Appl. Crystallogr. 38*, 398−400.
(78) Cherezov, V., and Caffrey, M. (2006) Picolitre-scale crystallization of membrane proteins. *J. Appl. Crystallogr. 39*, 604−606.
(79) Anachem/Gilson Flexus crystals IMP Robot (http://www.gilsonuk.com).
(80) Formulatrix NT8 LCP Robot (http://www.formulatrix.com).
(81) Gryphon LCP Robot (http://www.artrobbins.com).
(82) Zinsser Analytics ProCrys Meso Robot (http://www.zinsser-analytic.com).
(83) TTP Labtech Mosquito LCP (http://www.ttplabtech.com).
(84) Kubicek, J., Schlesinger, R., Baeken, C., Büldt, G., Schäfer, F., and Labahn, J. (2012) Controlled in meso phase crystallization: A method for the structural investigation of membrane proteins. *PLoS One 7*, e35458.
(85) Wallace, E., Dranow, D., Laible, P. D., Christensen, J., and Nollert, P. (2011) Monoolein lipid phases as incorporation and enrichment materials for membrane protein crystallization. *PLoS One 6*, e24488.
(86) Tate, C. G., and Stevens, R. C. (2010) Growth and excitement in membrane protein structural biology. *Curr. Opin. Struct. Biol. 20*, 399−400.
(87) Hanrahan, J. W., Gentzsch, M., and Riordan, J. R. (2003) The cystic fibrosis transmembrane conductance regulator (ABCC7). In *ABC proteins: From bacteria to man* (Holland, B., Higgins, C. F., Kuchler, K., and Cole, S. P. C., Eds.) pp 589−618, Elsevier Science Ltd., New York.
(88) Buchanan, S. K. (1999) β-Barrel proteins from bacterial outer membranes: Structure, function and refolding. *Curr. Opin. Struct. Biol. 9*, 455−461.
(89) Padan, E., Hunte, C., and Reilander, H. (2003) Production and purification of recombinant membrane proteins. In *Membrane protein purification and crystallization. A practical guide* (Hunte, C., Jagow, G. V., and Schagger, H., Eds.) pp 55−78, Academic Press, San Diego.
(90) Schwarz, D., Junge, F., Durst, F., Frolich, N., Schneider, B., Reckel, S., Sobhanifar, S., Dotsch, V., and Bernhard, F. (2007) Preparative scale expression of membrane proteins in *Escherichia coli*-based continuous exchange cell-free systems. *Nat. Protoc. 2*, 2945−2957.
(91) Yildiz, O., Vinothkumar, K. R., Goswami, P., and Kuhlbrandt, W. (2006) Structure of the monomeric outer-membrane porin OmpG in the open and closed conformation. *EMBO J. 25*, 3702−3713.
(92) Subbarao, G. V., and van den Berg, B. (2006) Crystal structure of the monomeric porin OmpG. *J. Mol. Biol. 360*, 750−759.
(93) Whitney, J. C., Hay, I. D., Li, C. H., Eckford, P. D. W., Robinson, H., Amaya, M. F., Wood, L. F., Ohman, D. E., Bear, C. E., Rehm, B. H., and Howell, P. L. (2011) Structural basis for alginate secretion across the bacterial outer membrane. *Proc. Natl. Acad. Sci. U.S.A. 108*, 13083−13088.
(94) Kawate, T., and Gouaux, E. (2006) Fluorescence-detection size-exclusion chromatography for precrystallization screening of integral membrane proteins. *Structure 14*, 673−681.

(95) Drew, D., Lerch, M., Kunji, E., Slotboom, D. J., and de Gier, J. W. (2006) Optimization of membrane protein overexpression and purification using GFP fusions. *Nat. Methods 3*, 303−313.
(96) Hsieh, J. M., Besserer, G. M., Madej, M. G., Bui, H. Q., Kwon, S., and Abramson, J. (2010) Bridging the gap: A GFP-based strategy for overexpression and purification of membrane proteins with intra and extracellular C-termini. *Protein Sci. 19*, 868−880.
(97) Bass, R. B., Strop, P., Barclay, M., and Rees, D. C. (2002) Crystal structure of *Escherichia coli* MscS, a voltage-modulated and mechanosensitive channel. *Science 298*, 1582−1587.
(98) Miller, J. L., and Tate, C. G. (2011) Engineering an ultra-thermostable β1-adrenoceptor. *J. Mol. Biol. 413*, 628−638.
(99) Zhou, Y. F., and Bowie, J. U. (2000) Building a thermostable membrane protein. *J. Biol. Chem. 275*, 6975−6979.
(100) Ely, L. K., Fischer, S., and Garcia, K. C. (2009) Structural basis of receptor sharing by interleukin 17 cytokines. *Nat. Immunol. 10*, 1245−1251.
(101) He, X. L., Dukkipati, A., and Garcia, K. C. (2006) Structural determinants of natriuretic peptide receptor specificity and degeneracy. *J. Mol. Biol. 361*, 698−714.
(102) Laver, W. G., Bischofberger, N., and Webster, R. G. (1999) Disarming flu viruses. *Sci. Am. 280*, 78−87.
(103) Thomas, C., Moraga, I., Levin, D., Krutzik, P. O., Podoplelova, Y., Trejo, A., Lee, C., Yarden, G., Vleck, S. E., Glenn, J. S., Nolan, G. P., Piehler, J., Schreiber, G., and Garcia, K. C. (2011) Structural linkage between ligand discrimination and receptor activation by type I interferons. *Cell 146*, 621−632.
(104) Barrera, N. P., Isaacson, S. C., Zhou, M., Bavro, V. N., Welch, A., Schaedler, T. A., Seeger, M. A., Miguel, R. N., Korkhov, V. M., van Veen, H. W., Venter, H., Walmsley, A. R., Tate, C. G., and Robinson, C. V. (2009) Mass spectrometry of membrane transporters reveals subunit stoichiometry and interactions. *Nat. Methods 6*, 585−587.
(105) Cohen, S. L., and Chait, B. T. (2001) Mass spectrometry as a tool for protein crystallography. *Annu. Rev. Biophys. Biomol. Struct. 30*, 67−85.
(106) Zhou, M., Morgner, N., Barrera, N. P., Politis, A., Isaacson, S. C., Matak-Vinkovic, D., Murata, T., Bernal, R. A., Stock, D., and Robinson, C. V. (2011) Mass spectrometry of intact V-type ATPases reveals bound lipids and the effects of nucleotide binding. *Science 334*, 380−385.
(107) Guan, L., Smirnova, I. N., Verner, G., Nagamoni, S., and Kaback, H. R. (2006) Manipulating phospholipids for crystallization of a membrane transport protein. *Proc. Natl. Acad. Sci. U.S.A. 103*, 1723−1726.
(108) Hunte, C., and Richers, S. (2008) Lipids and membrane protein structures. *Curr. Opin. Struct. Biol. 18*, 406−411.
(109) Zhang, H. M., Kurisu, G., Smith, J. L., and Cramer, W. A. (2003) A defined protein-detergent-lipid complex for crystallization of integral membrane proteins: The cytochrome b6f complex of oxygenic photosynthesis. *Proc. Natl. Acad. Sci. U.S.A. 100*, 5160−5163.
(110) Ferguson, A. D., Hofmann, E., Coulton, J. W., Diederichs, K., and Welte, W. (1998) Siderophore-mediated iron transport: Crystal structure of FhuA with bound lipopolysaccharide. *Science 282*, 2215−2220.
(111) Hanson, M. A., Cherezov, V., Griffith, M. T., Roth, C. B., Jaakola, V. P., Chien, E. Y., Velasquez, J., Kuhn, P., and Stevens, R. C. (2008) A specific cholesterol binding site is established by the 2.8 Å structure of the human β2-adrenergic receptor. *Structure 16*, 897−905.
(112) Rosenbaum, D. M., Zhang, C., Lyons, J. A., Holl, R., Aragao, D., Arlow, D. H., Rasmussen, S. G. F., Choi, H. J., DeVree, B. T., Sunahara, R. K., Chae, P. S., Gellman, S. H., Dror, R. O., Shaw, D. E., Weis, W. I., Caffrey, M., Gmeiner, P., and Kobilka, B. K. (2011) Structure and function of an irreversible agonist-β2 adrenoceptor complex. *Nature 469*, 236−240.
(113) Wacker, D., Fenalti, G., Brown, M. A., Katritch, V., Abagyan, R., Cherezov, V., and Stevens, R. C. (2010) Conserved binding mode of human β2 adrenergic receptor inverse agonists and antagonist revealed by X-ray crystallography. *J. Am. Chem. Soc. 132*, 11443−11445.
(114) Xu, F., Wu, H., Katritch, V., Han, G. W., Jacobson, K. A., Gao, Z. G., Cherezov, V., and Stevens, R. C. (2011) Structure of an agonist-bound human A2A adenosine receptor. *Science 332*, 322−327.
(115) Ballesteros, J. A., and Weinstein, H. (1995) Integrated methods for the construction of three-dimensional models and computational probing of structure-function relations in G protein-coupled receptors. *Methods Neurosci. 25*, 366−428.
(116) Roth, C. B., Hanson, M. A., and Stevens, R. C. (2008) Stabilization of the human β2-adrenergic receptor TM4-TM3-TM5 helix interface by mutagenesis of glu122(3.41), a critical residue in GPCR structure. *J. Mol. Biol. 376*, 1305−1319.
(117) Alexandrov, A. I., Mileni, M., Chien, E. Y. T., Hanson, M. A., and Stevens, R. C. (2008) Microscale fluorescent thermal stability assay for membrane proteins. *Structure 16*, 351−359.
(118) Serrano-Vega, M. J., Magnani, F., Shibata, Y., and Tate, C. G. (2008) Conformational thermostabilization of the β1-adrenergic receptor in a detergent-resistant form. *Proc. Natl. Acad. Sci. U.S.A. 105*, 877−882.
(119) Magnani, F., Shibata, Y., Serrano-Vega, M. J., and Tate, C. G. (2008) Co-evolving stability and conformational homogeneity of the human adenosine A2A receptor. *Proc. Natl. Acad. Sci. U.S.A. 105*, 10744−10749.
(120) Shibata, Y., White, J. F., Serrano-Vega, M. J., Magnani, F., Aloia, A. L., Grisshammer, R., and Tate, C. G. (2009) Thermostabilization of the neurotensin receptor NTS1. *J. Mol. Biol. 390*, 262−277.
(121) Lebon, G., Bennett, K., Jazayeri, A., and Tate, C. G. (2011) Thermostabilisation of an agonist-bound conformation of the human adenosine A2A receptor. *J. Mol. Biol. 409*, 298−310.
(122) Warne, T., Serrano-Vega, M. J., Tate, C. G., and Schertler, G. F. X. (2009) Development and crystallization of a minimal thermostabilised G protein-coupled receptor. *Protein Expression Purif. 65*, 204−213.
(123) Warne, T., Edwards, P. C., Leslie, A. G., and Tate, C. G. (2012) Crystal structures of a stabilized β1-adrenoceptor bound to the biased agonists bucindolol and carvedilol. *Structure 20*, 841−849.
(124) Dore, A. S., Robertson, N., Errey, J. C., Ng, I., Hollenstein, K., Tehan, B., Hurrell, E., Bennett, K., Congreve, M., Magnani, F., Tate, C. G., Weir, M., and Marshall, F. H. (2011) Structure of the adenosine A2A receptor in complex with ZM241385 and the xanthines XAC and caffeine. *Structure 19*, 1283−1293.
(125) Warne, T., Serrano-Vega, M. J., Baker, J. G., Moukhametzianov, R., Edwards, P. C., Henderson, R., Leslie, A. G. W., Tate, C. G., and Schertler, G. F. X. (2008) Structure of a β1-adrenergic G-protein-coupled receptor. *Nature 454*, 486−491.
(126) Ai, X., and Caffrey, M. (2000) Membrane protein crystallization in lipidic mesophases: Detergent effects. *Biophys. J. 79*, 394−405.
(127) Rigaud, J. L., Mosser, G., Lacapere, J. J., Olofsson, A., Levy, D., and Ranck, J. L. (1997) Bio-beads: An efficient strategy for two-dimensional crystallization of membrane proteins. *J. Struct. Biol. 118*, 226−235.
(128) Briggs, J. (1994) The phase behavior of hydrated monoacylglycerols and the design of an X-ray compatible scanning calorimeter. Ph.D. Thesis, The Ohio State University, Columbus, OH.
(129) Briggs, J., and Caffrey, M. (1994) The temperature-composition phase diagram and mesophase structure characterization of monopentadecenoin in water. *Biophys. J. 67*, 1594−1602.
(130) Briggs, J., and Caffrey, M. (1994) The temperature-composition phase diagram of monomyristolein in water: Equilibrium and metastability aspects. *Biophys. J. 66*, 573−587.
(131) Briggs, J., Chung, H., and Caffrey, M. (1996) The temperature-composition phase diagram and mesophase structure characterization of the monoolein/water system. *J. Phys. II 6*, 723−751.
(132) Qiu, H., and Caffrey, M. (1999) Phase behavior of the monoerucin/water system. *Chem. Phys. Lipids 100*, 55−79.
(133) Misquitta, L. V., Misquitta, Y., Cherezov, V., Slattery, O., Mohan, J. M., Hart, D., Zhalnina, M., Cramer, W. A., and Caffrey, M. (2004) Membrane protein crystallization in lipidic mesophases with tailored bilayers. *Structure 12*, 2113−2124.

(134) Cherezov, V., Clogston, J., Misquitta, Y., Abdel-Gawad, W., and Caffrey, M. (2002) Membrane protein crystallization in meso: Lipid type-tailoring of the cubic phase. *Biophys. J. 83*, 3393−3407.
(135) Wohri, A. B., Johansson, L. C., Wadsten-Hindrichsen, P., Wahlgren, W. Y., Fischer, G., Horsefield, R., Katona, G., Nyblom, M., Oberg, F., Young, G., Cogdell, R. J., Fraser, N. J., Engstrom, S., and Neutze, R. (2008) A lipidic-sponge phase screen for membrane protein crystallization. *Structure 16*, 1003−1009.
(136) Misquitta, Y., Cherezov, V., Havas, F., Patterson, S., Mohan, J. M., Wells, A. J., Hart, D. J., and Caffrey, M. (2004) Rational design of lipid for membrane protein crystallization. *J. Struct. Biol. 148*, 169−175.
(137) Lyons, J. A., Aragao, D., Slattery, O., Pisliakov, A. V., Soulimane, T., and Caffrey, M. (2012) Structural insights into electron transfer in caa_3-type cytochrome oxidase. *Nature*, DOI: 10.1038/nature11182.
(138) Li, D., Lee, J., and Caffrey, M. (2011) Crystallizing membrane proteins in lipidic mesophases. A host lipid screen. *Cryst. Growth Des. 11*, 530−537.
(139) Hato, M., Minamikawa, H., Salkar, R. A., and Matsutani, S. (2004) Phase behavior of phytanyl-chained akylglycoside/water systems. *Prog. Colloid Polym. Sci. 123*, 56−60.
(140) Luzzati, V. (1968) *Biological membranes, physical facts and function*, Academic Press, New York.
(141) Sharpe, H. J., Stevens, T. J., and Munro, S. (2010) A comprehensive comparison of transmembrane domains reveals organelle-specific properties. *Cell 142*, 158−169.
(142) Avanti Polar Lipids (http://www.avantilipids.com), Sigma-Aldrich (http://www.sigmaaldrich.com), Nu-Chek Prep (http://www.nu-chekprep.com).
(143) Qiagen (http://www.qiagen.com).
(144) Grabe, M., Neu, J., Oster, G., and Nollert, P. (2003) Protein interactions and membrane geometry. *Biophys. J. 84*, 854−868.
(145) Hofer, N., Aragao, D., and Caffrey, M. (2010) Crystallizing transmembrane peptides in lipidic mesophases. *Biophys. J. 99*, L23−L25.
(146) Nugent, T., and Jones, D. T. (2009) Transmembrane protein topology prediction using support vector machines. *BMC Bioinf. 10*, 159.
(147) Pye, V. E., Aragao, D., Lyons, J. A., and Caffrey, M. (2011) Overview of the 13th international conference on the crystallization of biological macromolecules. *Cryst. Growth Des. 11*, 4723−4730.
(148) ICCBM12 (2008) 12th international conference on biological macromolecules (ICCBM12), Cancun, Mexico, (http://www.iccbm12.com.mx).
(149) GPCR Workshop 2011, Maui, HI (http://www.gpcrworkshop.com).
(150) Australian Course in Macromolecular Crystallisation 2012, Melbourne, Australia (http://crystal.csiro.au/en/Events/%7E/media/8A1B891319B14FBA93D36416C63A8165.ashx).
(151) GPCR Workshop 2012, Tsinghua University, Beijing (http://www.cls.edu.cn/english/Academicactivities/notices/index1076.shtml).
(152) Kissick, D. J., Gualtieri, E. J., Simpson, G. J., and Cherezov, V. (2010) Nonlinear optical imaging of integral membrane protein crystals in lipidic mesophases. *Anal. Chem. 82*, 491−497.
(153) Aishima, J., Owen, R. L., Axford, D., Shepherd, E., Winter, G., Levik, K., Gibbons, P., Ashton, A., and Evans, G. (2010) High-speed crystal detection and characterization using a fast-readout detector. *Acta Crystallogr. D66*, 1032−1035.
(154) Hilgart, M. C., Sanishvili, R., Ogata, C. M., Becker, M., Venugopalan, N., Stepanov, S., Makarov, O., Smith, J. L., and Fischetti, R. F. (2011) Automated sample-scanning methods for radiation damage mitigation and diffraction-based centering of macromolecular crystals. *J. Synchrotron Radiat. 18*, 717−722.
(155) Chapman, H. N., Fromme, P., Barty, A., White, T. A., Kirian, R. A., Aquila, A., Hunter, M. S., Schulz, J., DePonte, D. P., Weierstall, U., Doak, R. B., Maia, F. R., Martin, A. V., Schlichting, I., Lomb, L., Coppola, N., Shoeman, R. L., Epp, S. W., Hartmann, R., Rolles, D., Rudenko, A., Foucar, L., Kimmel, N., Weidenspointner, G., Holl, P., Liang, M., Barthelmess, M., Caleman, C., Boutet, S., Bogan, M. J., Krzywinski, J., Bostedt, C., Bajt, S., Gumprecht, L., Rudek, B., Erk, B., Schmidt, C., Homke, A., Reich, C., Pietschner, D., Struder, L., Hauser, G., Gorke, H., Ullrich, J., Herrmann, S., Schaller, G., Schopper, F., Soltau, H., Kuhnel, K. U., Messerschmidt, M., Bozek, J. D., Hau-Riege, S. P., Frank, M., Hampton, C. Y., Sierra, R. G., Starodub, D., Williams, G. J., Hajdu, J., Timneanu, N., Seibert, M. M., Andreasson, J., Rocker, A., Jonsson, O., Svenda, M., Stern, S., Nass, K., Andritschke, R., Schroter, C. D., Krasniqi, F., Bott, M., Schmidt, K. E., Wang, X., Grotjohann, I., Holton, J. M., Barends, T. R., Neutze, R., Marchesini, S., Fromme, R., Schorb, S., Rupp, D., Adolph, M., Gorkhover, T., Andersson, I., Hirsemann, H., Potdevin, G., Graafsma, H., Nilsson, B., and Spence, J. C. (2011) Femtosecond X-ray protein nanocrystallography. *Nature 470*, 73−77.
(156) Fromme, P., and Spence, J. C. (2011) Femtosecond nanocrystallography using X-ray lasers for membrane protein structure determination. *Curr. Opin. Struct. Biol. 21*, 509−516.
(157) Johansson, L. C., Arnlund, D., White, T. A., Katona, G., Deponte, D. P., Weierstall, U., Doak, R. B., Shoeman, R. L., Lomb, L., Malmerberg, E., Davidsson, J., Nass, K., Liang, M., Andreasson, J., Aquila, A., Bajt, S., Barthelmess, M., Barty, A., Bogan, M. J., Bostedt, C., Bozek, J. D., Caleman, C., Coffee, R., Coppola, N., Ekeberg, T., Epp, S. W., Erk, B., Fleckenstein, H., Foucar, L., Graafsma, H., Gumprecht, L., Hajdu, J., Hampton, C. Y., Hartmann, R., Hartmann, A., Hauser, G., Hirsemann, H., Holl, P., Hunter, M. S., Kassemeyer, S., Kimmel, N., Kirian, R. A., Maia, F. R., Marchesini, S., Martin, A. V., Reich, C., Rolles, D., Rudek, B., Rudenko, A., Schlichting, I., Schulz, J., Seibert, M. M., Sierra, R. G., Soltau, H., Starodub, D., Stellato, F., Stern, S., Struder, L., Timneanu, N., Ullrich, J., Wahlgren, W. Y., Wang, X., Weidenspointner, G., Wunderer, C., Fromme, P., Chapman, H. N., Spence, J. C., and Neutze, R. (2012) Lipidic phase membrane protein serial femtosecond crystallography. *Nat. Methods 9*, 263−265.
(158) Fairman, J. W., Dautin, N., Wojtowicz, D., Liu, W., Noinaj, N., Barnard1, T. J., Udho, E., Przytycka, T. M., Cherezov, V., and Buchanan, S. K. (2012) Crystal structures of the outer membrane domain of intimin and invasin from enterohemorrhagic *E. coli* and enteropathogenic *Y. pseudotuberculosis*. *Structure 20*, 1233−1243.
(159) Kato, H. E., Zhang, F., Yizhar, O., Ramakrishnan, C., Nishizawa, T., Hirata, K., Ito, J., Aita, Y., Tsukazaki, T., Hayashi, S., Hegemann, P., Maturana, A. D., Ishitani, R., Deisseroth, K., and Nureki, O. (2012) Crystal structure of the channelrhodopsin light-gated cation channel. *Nature 482*, 369−374.
(160) Liao, J., Li, H., Zeng, W. Z., Sauer, D. B., Belmares, R., and Jiang, Y. X. (2012) Structural insight into the ion-exchange mechanism of the sodium/calcium exchanger. *Science 335*, 686−690.